How to cite:
doi.org/10.1002/anie.202219306

Catalysis

Single-Atom Catalysis in Organic Synthesis

*Vitthal B. Saptal[+], Vincenzo Ruta[+], Mark A. Bajada[+], and Gianvito Vilé**

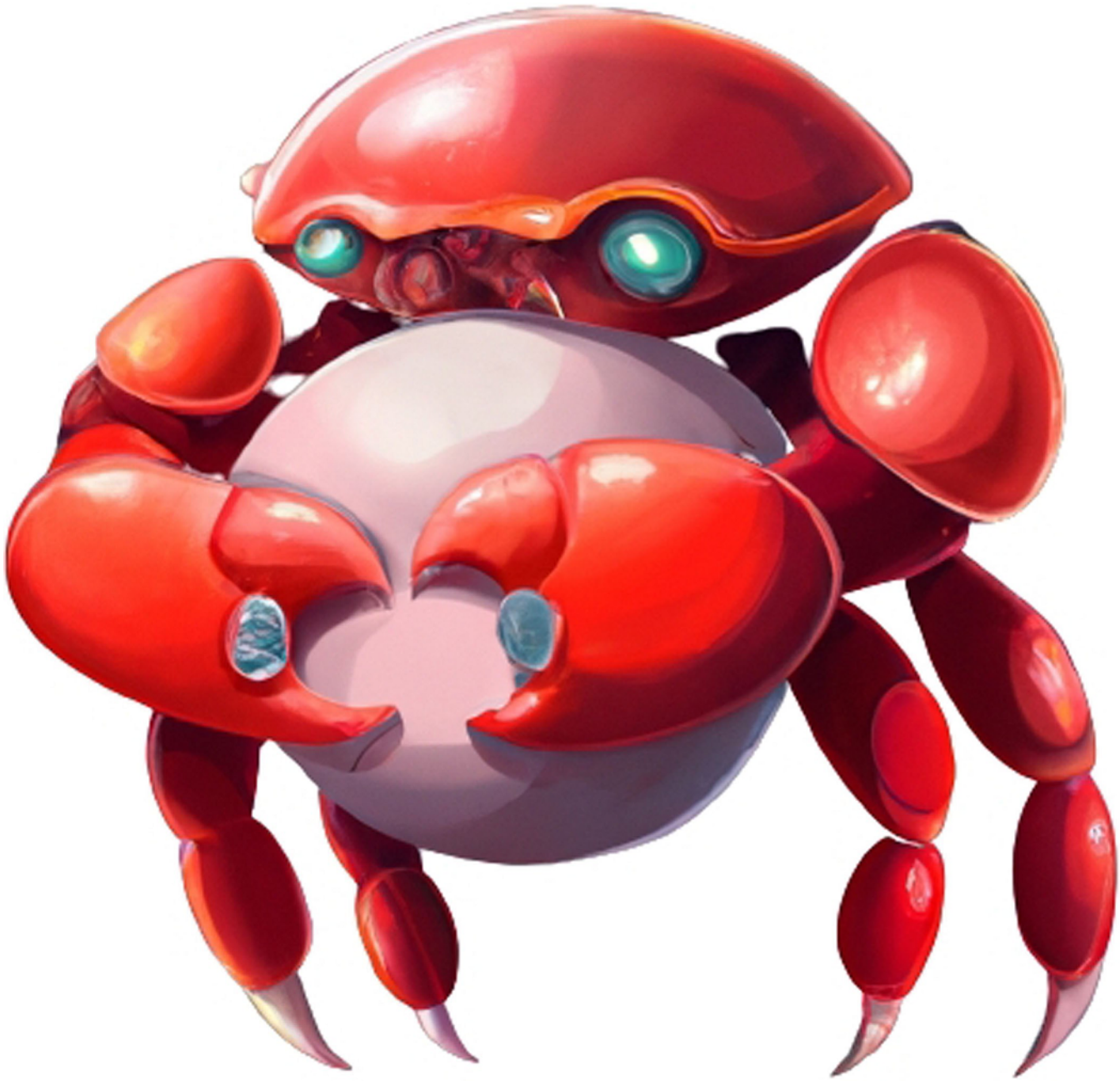

Angewandte International Edition Chemie

© 2023 The Authors. Angewandte Chemie International Edition published by Wiley-VCH GmbH

Abstract: Single-atom catalysts hold the potential to significantly impact the chemical sector, pushing the boundaries of catalysis in new, uncharted directions. These materials, featuring isolated metal species ligated on solid supports, can exist in many coordination environments, all of which have shown important functions in specific transformations. Their emergence has also provided exciting opportunities for mimicking metalloenzymes and bridging the gap between homogeneous and heterogeneous catalysis. This Review outlines the impressive progress made in recent years regarding the use of single-atom catalysts in organic synthesis. We also illustrate potential knowledge gaps in the search for more sustainable, earth-abundant single-atom catalysts for synthetic applications.

1. Introduction

Synthetic organic chemistry has historically been a powerful tool for preparing medicines, natural products, agrochemicals, polymers, among many other useful compounds. However, thinking about an organic reaction is very much synonymous with thinking about a certain catalyst. Catalysts play a central role in organic synthesis by efficiently making or breaking chemical bonds.[1] In particular, the catalysis landscape for synthesis spans between the exploitation of solid catalysts containing metal nanoparticles (such as the Lindlar Pd–Pb catalyst for stereoselective hydrogenation of alkynes) and molecularly-defined homogeneous organometallic complexes dissolved in organic media (such as the Wilkinson catalyst for selective hydrogenation of alkenes).[2] Despite the excellent activity and selectivity, the latter category has several drawbacks, including lengthy and costly ligand design, high sensitivity of the final material towards air and moisture, complex separation to ensure metal recovery, and challenges in terms of catalyst stability.[3] Researchers have tried to immobilize organometallic complexes on solid carriers to solve some or all of these technical issues.[4] Over the past decade, surface organometallic catalysis has demonstrated outstanding performance for various reactions due to intuitive mechanisms derived from the elementary steps of molecular chemistry. In particular, these systems have been postulated as a unifying concept to bridge organometallic and metal nanoparticle catalysis.[5]

An alternative approach to surface organometallic catalysis involves using single-atom catalysts (SACs) (Figure 1).[6] Here, atoms are directly entrapped via distance-dependent interactions onto the surface of a support without an additional (spectator) ligand. The solid support plays the same role that ligands play over homogeneous organometallic complexes, efficiently enabling charge transfer to the metal.[6] Support engineering is thus crucial for synthesizing stable SACs.[7] Common supports often include soft materials with high surface area and active anchoring groups, such as carbon nitrides, covalent and metal organic frameworks, and graphene layers.[8] Besides, by controlling the support structure, it becomes possible to regulate the surface free energy of the isolated atoms against aggregation and clustering.[9] The well-defined and spatially-ordered environment makes these systems very close to ligand-based organometallic systems.[10] Such a spatial definition is absent in traditional nanoclusters or particles due to the peculiar shape, size, and structural distribution of the active center.[11] As a result, each site in SACs is accessible and functional for the catalytic reaction, which is important to minimize the use of transition metals for reactions catalyzed over expensive and rare elements.[12] Excellent reviews cover the main features of these catalytic systems; reference is made to the articles by Yang et al.,[13] Wang et al.,[14] and Kaiser et al.[15] These reviews have highlighted that understanding the differences in the atomic structures and electronic states of SACs is important for improvements in the fabrication of these catalysts and for gaining fundamental insights into the origins of their catalytic activities.

The concept of solid materials with atomically-dispersed metals can be traced back to the 1970s, when Köpp et al.[16] conducted pioneering research on the first single-atom catalyst. Despite the significance of their work, the scientific community overlooked their contributions mainly due to the experimental challenge of visualizing atomically-dispersed sites with a microscope. The field saw a resurgence of interest in the 21st century when the development of new methods enabled the detection and characterization of atomically dispersed metals with an unprecedented resolution (Scheme 1a). To date, SACs have been reported for several synthetic transformations.[17] Nonetheless, even though the scientific community has broadened the use of such synthetic methods, published reviews have primarily focused on the effectiveness of SACs in activating small molecules, such as H_2, O_2, and CO_2.[18] Testament to this is the fact that no comprehensive review exists, which elegantly summarizes the application of SACs in complex organic transformations under liquid phase conditions.[5] A discussion on this critical aspect is therefore deemed essential, and complements our recent contribution to the exploitation of SACs for organic electrosynthesis.[19] Hence, this article summarizes the progress made using SACs in organic synthesis, covering a wide variety of substrates and reaction mechanisms (Scheme 1b).

The review begins by introducing the science of single-atom catalysis and presenting case studies where these

[*] Dr. V. B. Saptal,[+] V. Ruta,[+] Dr. M. A. Bajada,[+] Prof. Dr. G. Vilé
Department of Chemistry, Materials, and Chemical Engineering "Giulio Natta", Politecnico di Milano
Piazza Leonardo da Vinci 32, 20133 Milano (Italy)
E-mail: gianvito.vile@polimi.it

[+] These authors contributed equally to this work.

© 2023 The Authors. Angewandte Chemie International Edition published by Wiley-VCH GmbH. This is an open access article under the terms of the Creative Commons Attribution License, which permits use, distribution and reproduction in any medium, provided the original work is properly cited.

materials were applied in organic synthesis. Those are categorized based on reaction type (i.e., oxidation, C–C, C–N and C–O coupling, hydrogenation/reduction, hydroelementation, cycloaddition, hydroformylation). This approach is useful to organic chemists wishing to reproduce specific reaction types, in order to understand the generality of the method and the substrate tolerance. These sections are followed by a critical (data-driven) evaluation of the type of metals and carriers used in all synthetic reactions, and the routes to design such optimal catalysts. The concluding part is more didactic in style, to help the reader recognize the untapped opportunities of metal single-atom catalysis in organic synthesis.

2. Preparation and characterization of SACs

SACs can be made using different methods, which are often classified as the "bottom-up" or "top-down" approach.[20] "Bottom-up" procedures exploit chemical reactions among atoms, ions, and molecules to "construct" a catalyst with atomically-isolated sites. Methods such as wet chemistry, atomic layer deposition, chemical vapor deposition, or electrochemical synthesis can be used for this purpose. The properties of the final catalyst are controlled by adjusting the concentration of the atoms, ions, and molecules, the pH, temperature, and reaction time. Alternatively, "top-down" techniques involve energy-related methods to "crush" and "break" a large metal structure (e.g., a supported metal nanoparticle) into individual and isolated atoms, without affecting the structure of support.[21] Mechanochemical and photochemical methods, laser ablation, or pyrolysis are among the methods that can be used to achieve this. In all cases, the chosen synthetic route always depends on a trade-off between availability of reagents and setups.[22] Some of the most practiced approaches are summarized below for clarity.

Wet chemistry methods. This is a quintessential example of a "bottom-up" method; the support is typically immersed in an aqueous solution of the metal precursor, which can be a metal salt or an organometallic complex. Molecular hydrogen or a chemical reducing agent is then added to reduce the metal precursor and deposit it in the form of individual atoms onto the support. An example of this method was developed by Li et al. for the synthesis of $Pt_1@Ni(OH)_x$ SACs, and was subsequently used for the diboration of alkynes and alkenes.[23]

Atomic layer deposition (ALD). This is another "bottom-up" method. The support is exposed to a series of alternating metal precursor and reactive gas pulses in a reaction chamber. Each pulse allows for the physical adsorption of a metal layer. The process is repeated until the desired metal loading and thickness is achieved. The metal precursor is typically a volatile compound, such as a metal halide or a metal alkoxide. For example, Lu et al. used ALD to deposit Pd_1 and Pt_1 single atoms on 2D black phosphorous.[24]

Chemical vapor deposition (CVD). This "bottom-up" method, instead, exploits the use of a metal precursor, which is injected into a reaction chamber, whereupon it reacts with a surface to form a thin film. Deposition of single atoms can be achieved by carefully controlling the temperature, pressure, and flow rates in the reaction chamber. For

Vitthal is a Marie Skłodowska-Curie postdoctoral fellow in the Vilé group at Politecnico di Milano, and joined in 2023. He received a PhD in Catalysis from the Institute of Chemical Technology Mumbai in 2019. Then, he had postdoctoral appointments in various institutes in South Korea, China, India, and Poland. His research interests include the design of homogeneous and heterogeneous catalysts and their applications in organic synthesis.

Vincenzo is a PhD student in the Vilé group at Politecnico di Milano, and joined in 2021. He received a MSc in pharmaceutical chemistry from the University of Bari. His current research interests target the development of batch and continuous synthetic methodologies exploiting single-atom catalysts.

Mark is a Marie Skłodowska-Curie postdoctoral fellow in the Vilé group at Politecnico di Milano, and joined in 2021. He holds a BSc in chemistry and physics from the University of Malta, and a MPhil in energy engineering from the University of Cambridge. He received a PhD from the University of Cambridge, with a thesis on photo- and electrocatalysis under Prof. Erwin Reisner's supervision, funded through the Endeavour Scholarship. His current research tackles the design of sustainable processes based on single-atom catalysts.

Gianvito is an associate professor of chemical engineering at Politecnico di Milano. He received his PhD from ETH Zurich and, from 2016 to 2019, was lab head in chemistry technologies at Idorsia Pharmaceuticals. His research focuses on understanding the structure and reactivity of single-atom catalysts. For his research, he has received the ETH medal, the Dimistris N. Chorafas award, the Felder award, the ERC Starting Grant, and the Alfredo Di Braccio Prize from the National Italian Academy (Accademia dei Lincei).

© 2023 The Authors. Angewandte Chemie International Edition published by Wiley-VCH GmbH

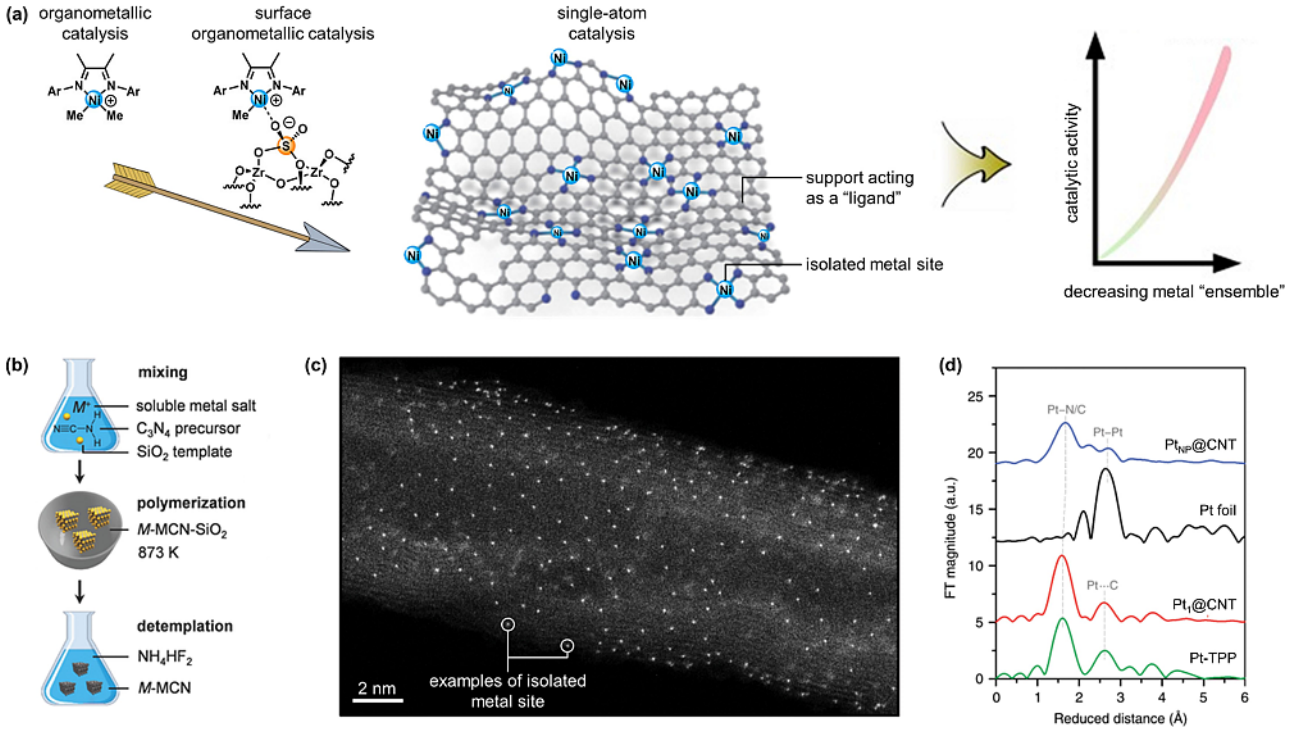

Figure 1. (a) Evolution of catalysis concepts in organic synthesis, from homogeneous organometallic chemistry to the emerging field of single-atom catalysis. On the side, it is shown the importance of decreasing the metal ensemble compared to conventional nanoparticle-based heterogeneous catalysts to enhance the catalytic activity. (b) Exemplary sketch for the preparation of a class of SACs. For a deeper study of all other possibilities to make SACs, the reader is directed to more specialized articles on the synthesis and characterization of SACs. (c) Aberration-corrected high-angle annular dark-field scanning transmission electron microscopy imaging of a single-atom Pt_1@CNT catalyst. The individual dots in the micrographs represent the isolated metal sites. (d) k^3-weighted Pt L3-edge extended X-ray absorption fine structure spectra of Pt_1@CNT and comparative Pt-based reference catalysts based on metal nanoparticles (Pt_{NP}@CNT), organometallic complexes (Pt-TPP), and foil (Pt foil). The absence of Pt–Pt bonds on the Pt_1@CNT spectra is demonstrated. Copyrights from Wiley and Nature Publishing Group.

example, CVD was demonstrated by Wu et al. to prepare a class of Fe-based SACs.[25]

Electrochemical synthesis. The metal precursor is dissolved in an electrolyte solution, and the support is used as the electrode. When an appropriate potential difference is applied across the cell, and current is passed through the electrolyte solution, the metal salt is reduced and deposited onto the surface of the support. For instance, Chen et al. used this strategy to design Cu SACs on the sulfur sites of a doped graphite foam.[26]

Mechanochemical method. This "top-down" technique uses high-energy ball milling to break apart metal nanoparticles and disperse the resulting metal atoms on a support. An example of this mechanochemical technique was reported by Ji et al. to synthesize Au_1@CeO_2.[27]

Pyrolysis process. This "top-down" method breaks supported metal nanoparticles into SACs by high-temperature treatment. Li et al., for example, found that above 900 °C, nanoparticles of noble metals (e.g., Pd, Pt, Au) can be broken into thermodynamically-stable single atoms.[28]

Photochemical method. In the photochemical synthesis of SACs, light is used as an energy source to induce chemical transformations in a photosensitive precursor, resulting in the deposition of single atoms on the support. A noteworthy demonstration of this approach was performed by Zheng et al. to create the Pd_1@TiO_2 SACs.[29]

The materials obtained can be then characterized by a combination of techniques, as summarized in Table 1. Such characterization methods are needed to probe the single-atom nature of the materials prepared through the aforementioned approaches.

3. Thermally driven organic synthesis using SACs

3.1. Oxidations

Selective oxidations are widely used in synthetic chemistry.[30] Although a broad range of transformations can be included in this definition, oxidation reactions can be considered as the introduction of a heteroatom (typically oxygen) on a reaction center, with the change of the oxidation state of this heteroatom. Conventional methods exploit stoichiometric amounts of toxic metal salts (e.g., chromates and CrO_3), oxidizing agents (e.g., $KMnO_4$, H_2O_2, Cl_2, O_2, O_3, $NaNO_3$), and precious metals (e.g., Pt, Pd, Rh-based catalysts). These conditions generate copious amounts of highly contaminated waste.[31] In recent years, SACs made

© 2023 The Authors. Angewandte Chemie International Edition published by Wiley-VCH GmbH

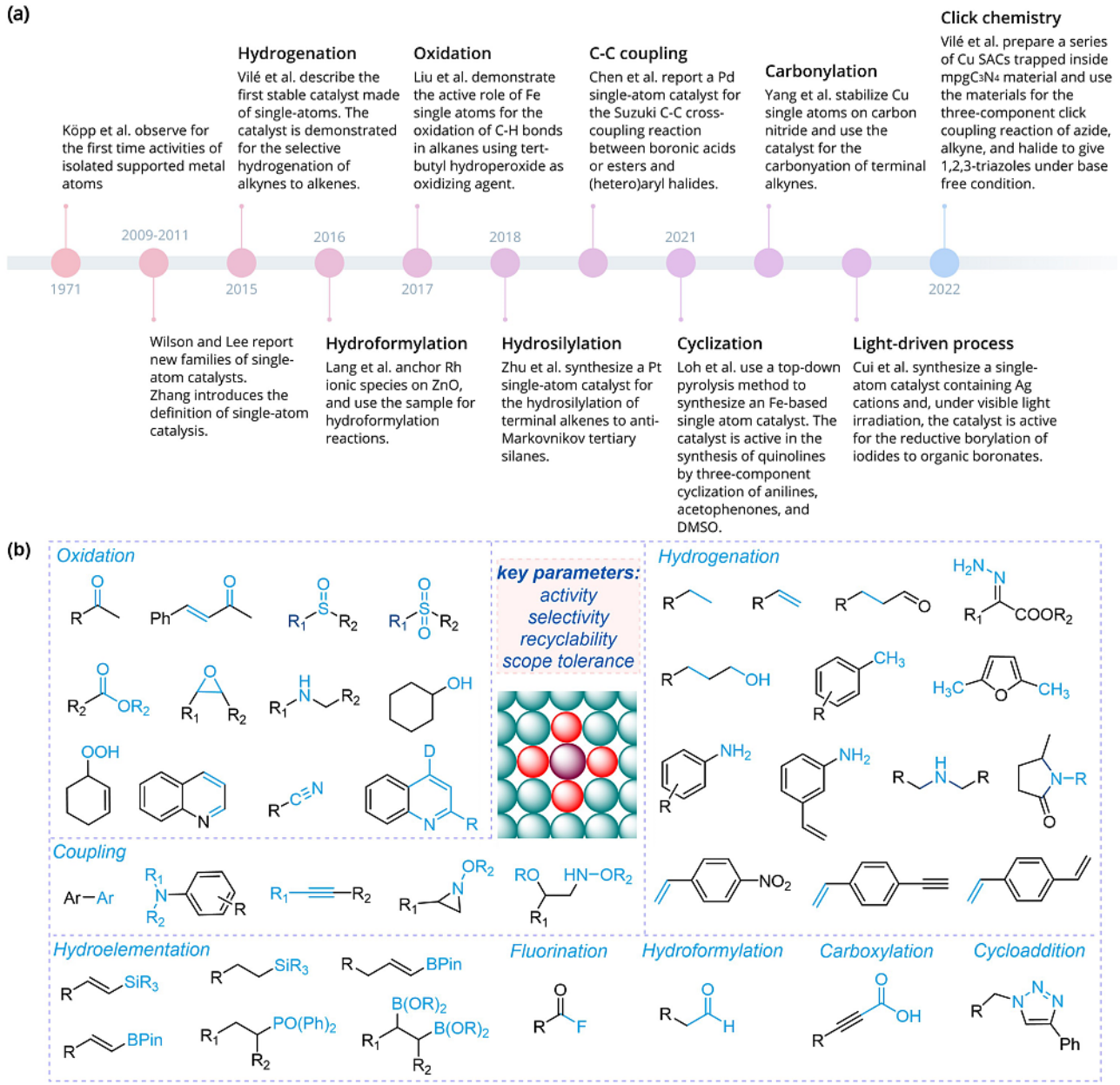

Scheme 1. (a) Chronological representation of the historical progression of synthetic processes based on single-atom catalysts (SACs). The initial synthetic application for each reaction class is indicated, and references to relevant works can be found in [16, 33, 44, 54, 55, 58, 68, 89, 93, 100]. (b) Overview of the various synthetic products currently achievable via SACs.

of precious and non-precious metals have been explored for the oxidation of various organic substrates.[32]

The pioneering work originated in 2017, when Liu et al. synthesized highly dispersed Fe sites using $Fe(phen)_x$ (phen = 1,10-phenanthroline) complex on N-doped carbon (denoted as Fe_1@N-doped C, Scheme 2).[33] The material was treated at 600, 700, and 800 °C. This Fe-based single-atom catalyst demonstrated excellent catalytic activity, selectivity, and stability for the oxidation of the C–H bond of alkanes using *tert*-butyl hydroperoxide (TBHP) as the oxidizing reagent at room temperature. Various alkanes with electron donating and withdrawing groups were tolerated, achieving 62–99 % isolated yields. A reaction mechanism was proposed based on a combination of experimental pieces of evidence and theoretical calculations. Initially, TBHP is adsorbed and activated at the Fe and N center of the catalyst. Activated ethylbenzene is formed from the adsorption of the catalyst with N donor ligands via hydrogen bonding. Then, the α-H is abstracted by *t*BuO• radical and generates an α-ethylbenzene radical, which reacts rapidly with radical of •OH to yield 1-phenylethyl alcohol. *t*BuO• removes H from the hydroxyl group, which forms 1-ethylbenzene oxygen radical, and this reacts with •OH radical to afford 1-hydroperoxyethylbenzene. Finally, elimination of water from 1-hydroperoxyethylbenzene yields the ketone product.

© 2023 The Authors. Angewandte Chemie International Edition published by Wiley-VCH GmbH

Table 1: Principal techniques for the characterization of SACs.

Technique	Scope
X-ray diffraction (XRD)	Crystallinity and phase purity of the material; check whether metal clusters or nanoparticles are present.
Elemental analysis	Loading of metal and composition of the support.
N_2 or Ar physisorption	Surface area and porosity.
Solid-state nuclear magnetic resonance (NMR)	Anchoring coordination of the isolated metals.
X-ray photoelectron spectroscopy (XPS)	Valence and bonding state of the atomic species composing the materials.
Aberration-corrected scanning transmission electron microscopy (STEM)	Angstrom-scale visualization of the atomic dispersion of the metal sites; determination of metal cluster dimension.
Energy dispersive spectroscopy (EDX)	Mapping of metal single-site dispersion throughout the material surface.
X-ray absorption spectroscopy (XAS)	Local coordination environment of metal atom, metal oxidation state, presence of metal-metal bonds (indicating possible non-single atom sites).
UV/Vis spectroscopy	Material light absorption peak; heterojunction type elucidation; band gap energy value (for photocatalysis)
Ultraviolet photoelectron spectroscopy (UPS)	Valence band energy level (for photocatalysis).
Photoluminescence (PL)	Electronic structure; band gap energy value (for photocatalysis).
H_2 temperature programmed reduction (TPR)	Reducibility of the metallic single atom sites.
Electron Paramagnetic Resonance (EPR)	Nature, symmetry, electronic structure, and changes in the valence states of the paramagnetic single metal center.
Cyclic voltammetry (CV)	Calculation of redox potentials (for photo- and electrocatalysis).

A further development of this class of materials was presented in 2019, when Zhou et al. synthesized SACs based on Fe, Co, Ni, and Cu, supported on N-doped carbon. The materials were used for the oxidative esterification of alcohols and aldehydes in the presence of molecular oxygen as an oxidant (Scheme 3).[34] The cobalt-based catalyst, however, was most effective, and provided higher isolated yields (60–100 %) and a stable catalytic performance for multiple (eight) catalytic cycles.

Taking advantage of the ability of Co to promote oxidation reactions, Chen et al. synthesized Co single atoms intercalated inside molybdenum disulfide nanosheets (MoS_2) (Scheme 4).[35] This catalyst was used for the oxidation of sulfides to sulfones and sulfoxides, using H_2O_2 as the oxidant. Various sulfides were oxidized chemoselectively over other subunits that included ketones, aldehydes, allyls, alcohols, amines, alkynes, and boronic esters. Additionally, the material demonstrated recyclability for five catalytic cycles. A reaction mechanism was proposed based on DFT calculations, which suggested that sulfide adsorption at the edge of Co single atom is the key step to enable a high chemoselectivity.

Another development in this area was presented by Qi et al., who synthesized SACs made of Co atoms ligated to 1,10-phenanthroline and deposited on silica gel (Scheme 5).[36] These catalysts were investigated for the epoxidation of plant oils, including camellia, sunflower, grape seed, and methyl ricinolate, using molecular oxygen as an oxidant and *n*-butyraldehyde as a reaction mediator. Based on kinetic and electron paramagnetic resonance (EPR) studies, a reaction mechanism was proposed. Initially, oxygen was adsorbed and activated on the Co site, and the adsorbate subsequently reacted with butyraldehyde to form a butyric acid peroxide intermediate, which underwent epoxidation of the double bond to give the final epoxide product.

Xu et al. instead synthesized Co SACs supported on spherical porous nanosilica, via pyrolysis of a metal-doped 1,10-phenanthroline ligand (Scheme 6).[37] This material was used for the oxidative dehydrogenation of heteroarenes using O_2 as an oxidant. The sample presented an excellent activity for the transfer hydrogenation of heteroarenes using formic acid as a reducing agent, with a turnover frequency (TOF) 25 times higher than that of the reference homogeneous catalyst.

An interesting example of innovative catalyst design, employing several valence states of the metal atoms, was proposed by Bakandritsos et al.[38] Here, the authors investigated the use of a mixed valence Cu^+/Cu^{2+} single-atom catalyst for the dehydrogenation of amines to imines (Scheme 7). The catalyst was active and selective towards several differently substituted amines in both the homocou-

© 2023 The Authors. Angewandte Chemie International Edition published by Wiley-VCH GmbH

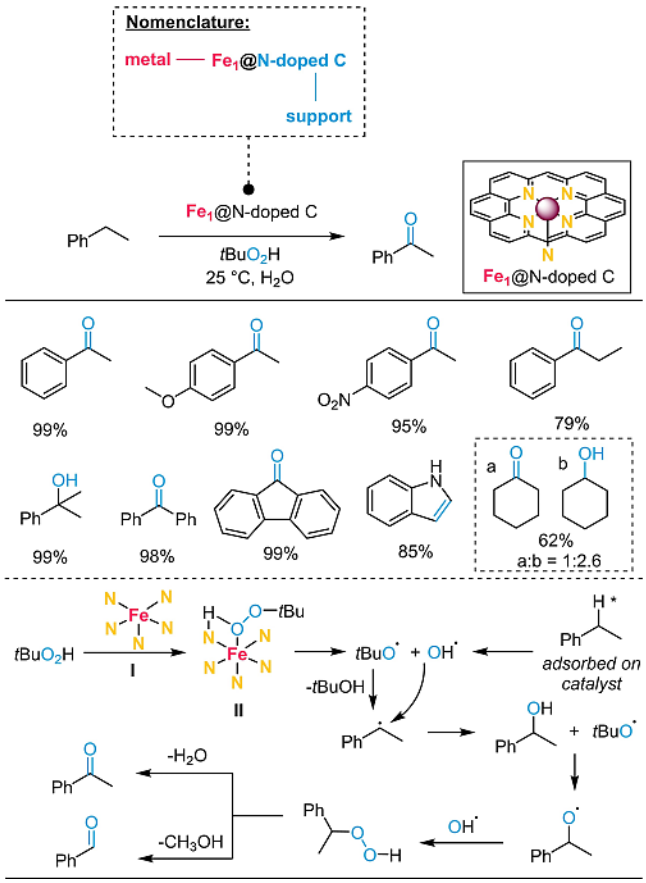

Scheme 2. Oxidation of C–H bond of alkanes catalyzed by Fe single-atom catalyst. Adapted from ref. [33].

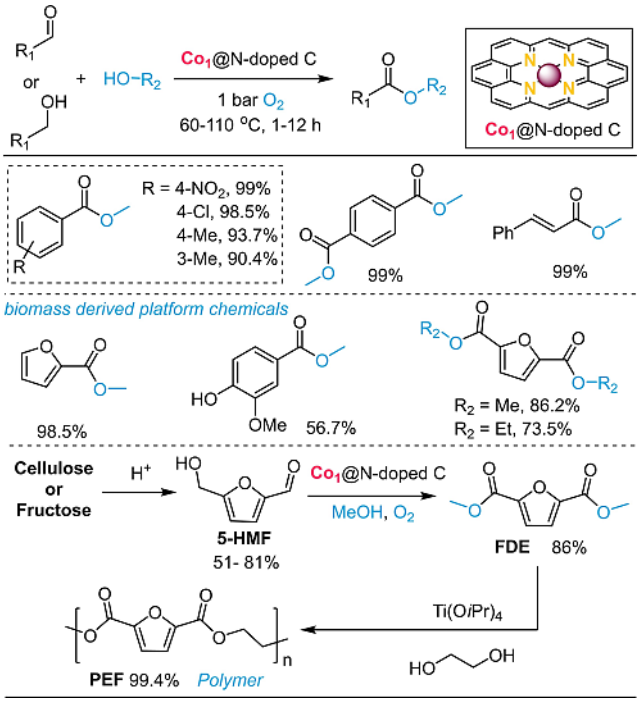

Scheme 3. Oxidative esterification catalyzed by Co single-atom catalyst. Adapted from ref. [34].

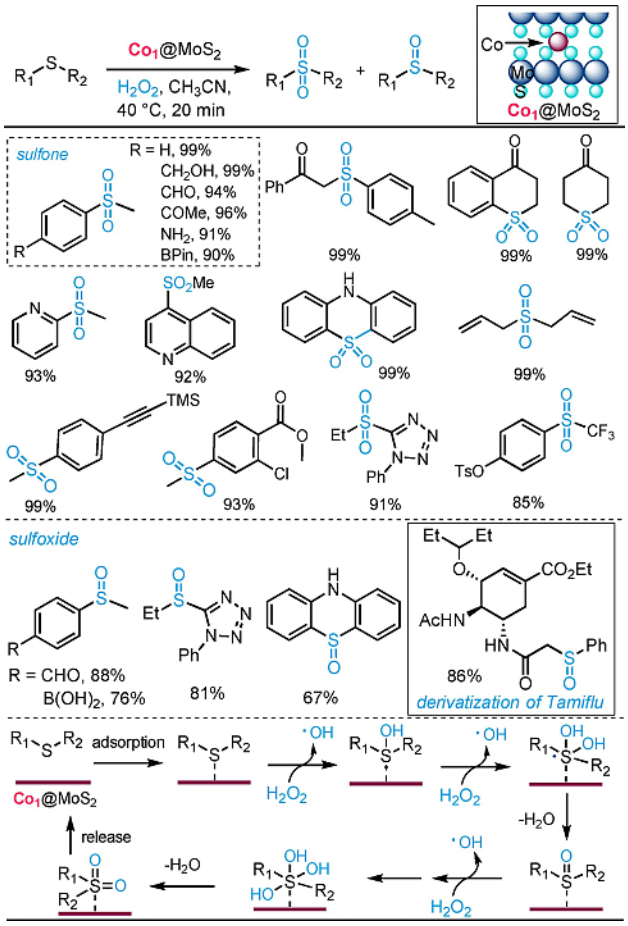

Scheme 4. Oxidation of sulfides catalyzed by Co single-atom catalyst. Adapted from ref. [35].

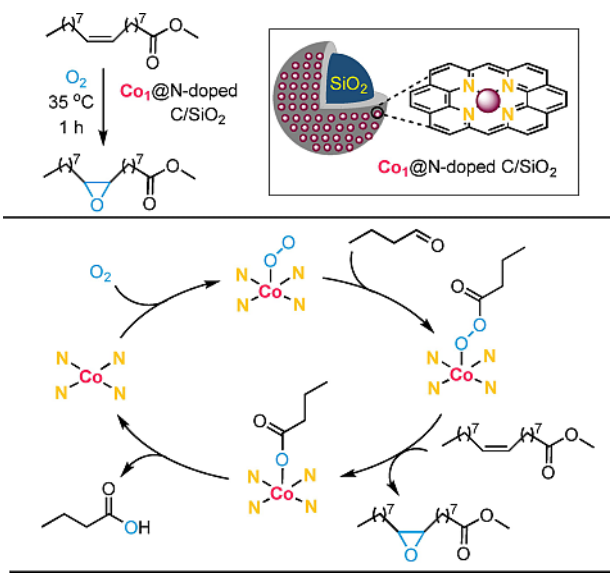

Scheme 5. Alkenes epoxidation over Co single-atom catalyst. Adapted from ref. [36].

© 2023 The Authors. Angewandte Chemie International Edition published by Wiley-VCH GmbH

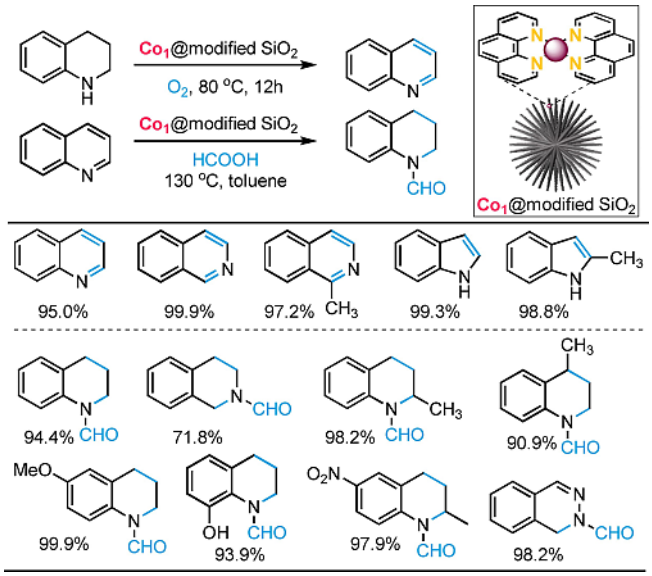

Scheme 6. Oxidative dehydrogenation of heteroarenes over a Co single-atom catalyst. Adapted from ref. [37].

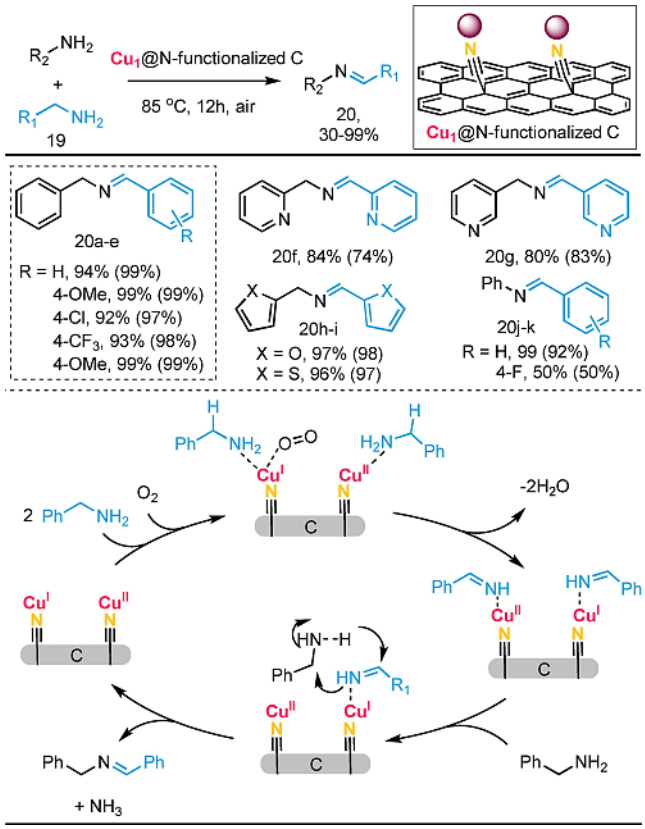

Scheme 7. Imine synthesis catalyzed by a Cu single-atom catalyst. Adapted from ref. [38].

pling and heterocoupling reaction, achieving 30–99 % isolated yields. Mechanistic studies via DFT calculations and EPR spectroscopy elucidated the importance of the synergistic role of the different Cu species, for both the adsorption of the reactants, and subsequent reaction mechanism.

An alternative approach was proposed by Büker et al., who deposited Cu single atoms on a graphitic carbon nitride (gC_3N_4) material, using Cu-EDTA as a precursor, following a two-step thermal method (Scheme 8).[39] This catalyst showed excellent activity for the liquid-phase cyclohexene oxidation using O_2 as an oxidant. The oxidation state of Cu was Cu^+, and this site was linearly coordinated to the N atoms of two gC_3N_4 layers. The activity of this single-atom catalyst was similar to the homogeneous reference Cu^I, but the heterogeneous nature of the material greatly simplified catalyst recovery.

Although Fe is the most used metal for oxidation catalysis, it is surprising to note that this metal has rarely been used as a single atom structure for organic synthesis. One of the few case studies was presented by Sun et al., where they employed a benzylamine-modified zeolitic imidazolate framework (ZIF) of Fe as the precursor for synthesizing an Fe single-atom catalyst (Scheme 9).[40] This catalyst was used to prepare nitriles by ammoxidation of alcohols with ammonia at 35 °C, using air as an oxidant. The protocol afforded a library of challenging nitriles, including compounds with phenyl benzylic, heterocyclic, allylic, and aliphatic substituents.

Another important example was shown by Li et al., who prepared MoS_2 nanosheets containing Fe single atoms (Scheme 10).[41] The catalyst was used to oxidize primary and secondary alcohols to the corresponding aldehydes and ketones, respectively, with a TOF up to 2105 h^{-1}. A wide range of aldehydes and ketones with aromatic, aliphatic, and heterocyclic functionalities were obtained, and the catalyst showed recyclability for several runs.

Pd SACs have also been widely exploited for oxidative reactions, likely due to the broad availability of synthetic methods to produce single-atom catalysts containing expensive noble metals, such as Pt and Pd. An example is given by Tiburcio et al., that observed an in situ generation of Pd single-atom sites during the aerobic oxidation of benzyl alcohols to carboxylic acids in the presence of molecular O_2 (Scheme 11).[42] A soluble metal organic framework (MOF)

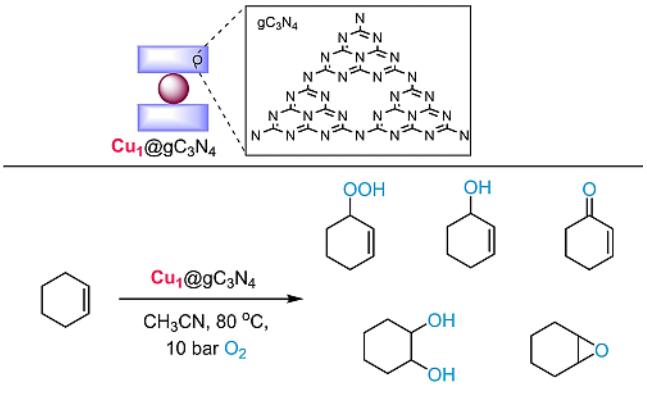

Scheme 8. Cyclohexene oxidation catalyzed by a Cu single-atom catalyst. Adapted from ref. [39].

© 2023 The Authors. Angewandte Chemie International Edition published by Wiley-VCH GmbH

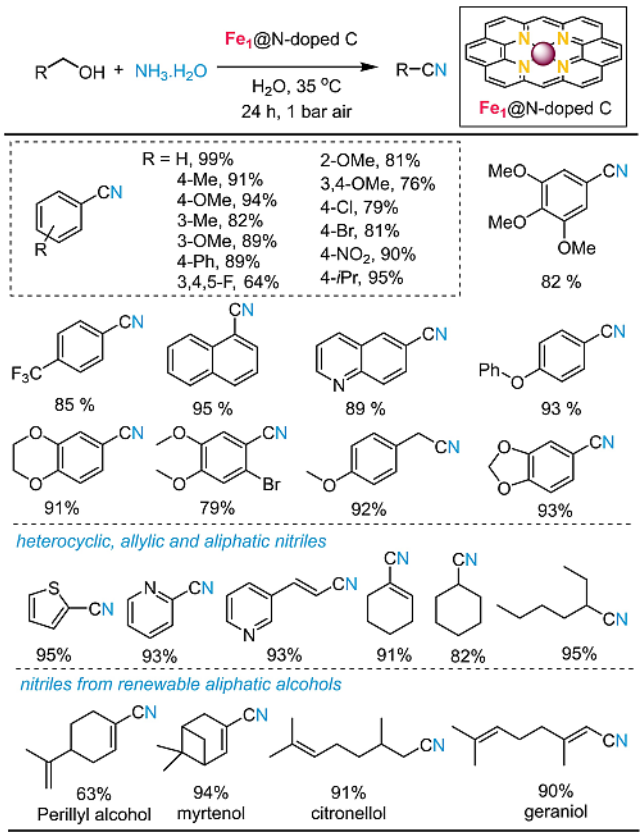

Scheme 9. Alcohol ammoxidation catalyzed by Fe single-atom catalyst. Adapted from ref. [40]

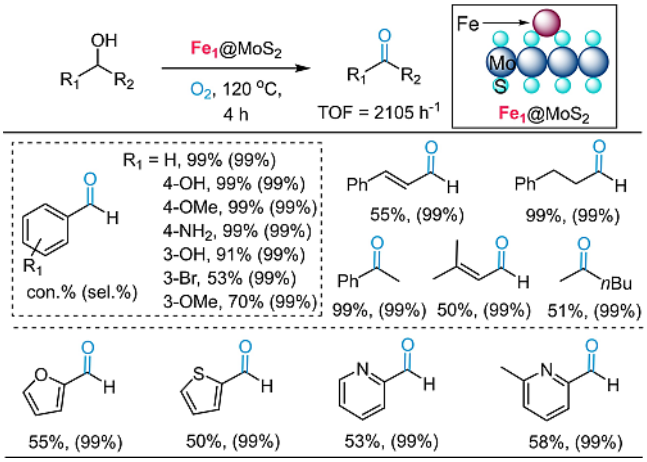

Scheme 10. Oxidation of alcohols catalyzed by a Fe single-atom catalyst. Adapted from ref. [41].

comprising methylcysteine-based ligand (MOF-5) was used to stabilize the single atoms of Pd.

3.2. C–C, C–N, and C–O couplings

Transition metal-catalyzed coupling reactions generate C–N, C–O, and C–C bonds. The catalytic cycle of a cross-coupling

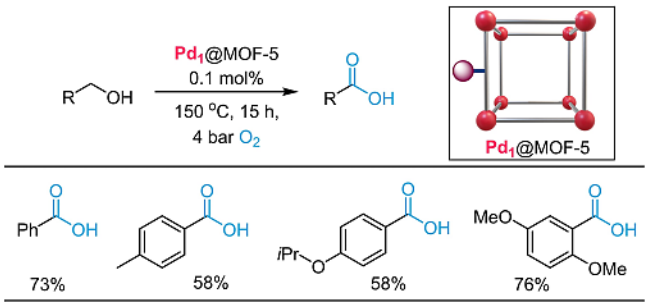

Scheme 11. Oxidation of alcohols to carboxylic acids over a Pd single-atom catalyst. Adapted from ref. [42].

reaction, in which the reactive center is a transition metal, involves a sequence of steps, including oxidative addition of the electrophile (a halide or pseudohalide), transmetallation in the presence of a C/N/O nucleophile, and reductive elimination of the product. Due to their reactivity, Pd complexes are the preferential choice for these reactions. Therefore, it is not surprising that most applications of SACs for C–N, C–O, and C–C bond constructions are based on the use of this particular metal. Nevertheless, examples reporting the use of other transition metals, including Ni and Cu, are present in the literature. The nature of the halide/pseudohalide group and the metal coordination influence the catalytic performance.

Over recent years, SACs have shown catalytic activity and selectivity in the same order of magnitude as their homogeneous analogue. This has been made possible by the application of rational catalyst design, and in exploiting metal-support interactions and interface confinement effects in order to maximize the activity of the single sites. Moreover, the continual advancements in preparative methods has allowed for the attainment of more stable and active catalysts for this class of organic transformations, with a particular focus on the well-known Suzuki C–C cross coupling reaction.[43] For example, Chen et al. synthesized Pd single atoms supported on exfoliated graphitic carbon nitride and used the material for the Suzuki C–C cross-coupling reaction, in which boronic acid or esters with (hetero)aryl halides are combined in the presence of a base (Scheme 12).[44] A wide range of challenging substrates of bromoarenes and phenylboronates were tolerated at mild conditions and with exceptional TOF (549 h^{-1}), which surpassed well-known homogeneous catalysts (e.g., the well-known tetrakis(triphenylphosphine)palladium catalyst gave a TOF of only 60 h^{-1} under the same reaction conditions). Additionally, the catalyst showed no signs of metal leaching during catalysis. A reaction mechanism was proposed, where the Pd atomic site adsorbs bromobenzene and phenylboronic acid, leading to Br^- displacement and generation of the C–C bond.

This seminal work was reproduced by Ding et al., who instead used ZnO–ZrO_2 as a mixed oxide support to develop a Pd-based single-atom material. Their work highlighted the advantages and role of a bimetallic oxide support for the stabilization of Pd single atoms. This catalyst was

© 2023 The Authors. Angewandte Chemie International Edition published by Wiley-VCH GmbH

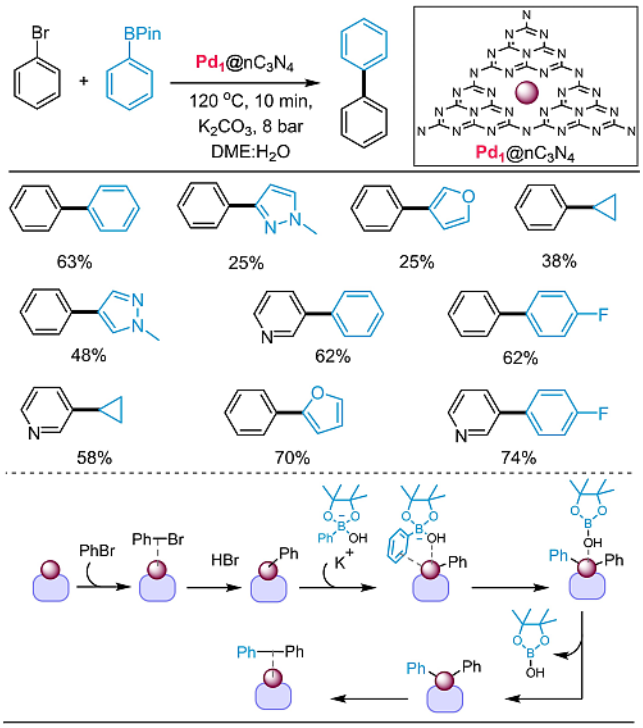

Scheme 12. Suzuki cross-coupling reaction catalyzed by a Pd single-atom catalyst. Adapted from ref. [44].

used for the Suzuki–Miyaura C–C bond coupling reaction at room temperature (Scheme 13).[45]

Jin et al. further explored the advantage of using a defective oxide (i.e., titania, anatase crystal form) for stabilizing Pd single atoms via charge transfer.[46] This catalyst demonstrated an excellent catalytic function in the Suzuki reaction at room temperature, corroborating the previous results. A TOF up to 11,000 h^{-1} with a wide range of substrates was achieved. The activity of the catalyst exceeded the homogeneous references, such as $PdCl_2$ and $Pd(OAc)_2$, by a factor of >200. Finally, Liu et al. synthesized a two-dimensional Pd catalyst based on the N_3C_1 structure of metal-porphyrin (Scheme 14).[47] This catalyst also offered optimal catalytic activity for the Suzuki coupling reaction for various substrates, achieving 99 % isolated yield in all cases. The single-atom catalyst was also applied to synthesize indomethacin, an anti-inflammatory drug. Overall, these publications demonstrate that Pd SACs are highly active and selective materials for Suzuki cross coupling chemistry, independent of the specific support used to stabilize the individual metal atoms.

Pd-based organometallic catalysts are also widely employed for other types of C–C cross couplings. For example, Zhang et al. used TiO_2 nanoparticles as a support for anchoring Pd single atoms, and applied the material in the Sonogashira C–C coupling reaction, a classic Pd-catalyzed cross-coupling in which terminal alkynes react with aryl or vinyl halides in the presence of a base. Here, substituted phenylacetylenes could be synthesized under mild conditions using ethanol as solvent (Scheme 15).[48] DFT calculations demonstrated that Pd single atoms coordinated to the surface lattice oxygen atoms of TiO_2 chemisorb iodobenzene to produce a phenyl intermediate, which then couples phenylacetylene to lead to the diphenylacetylene product.

Hu et al. investigated the effect of (100) and (111) facets of CeO_2 as a support for stabilizing Pd single atoms (Scheme 16).[49] In particular, the characterization showed that on CeO_2(100), isolated metal species were preferentially obtained on oxygen vacancies, i.e., sites on the catalyst surface where oxygen was missing, while on CeO_2(111) Pd

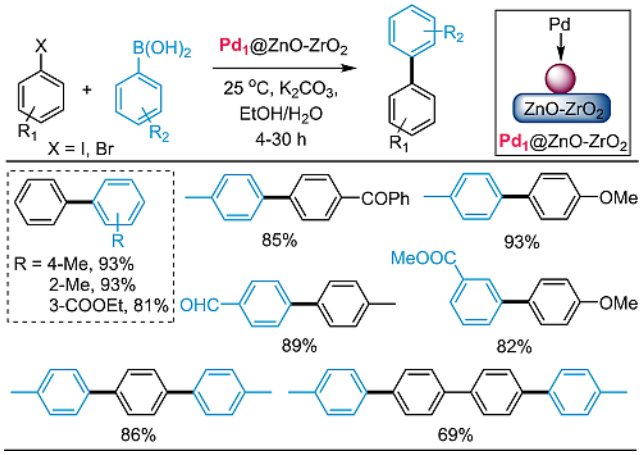

Scheme 13. Suzuki coupling performed over a Pd single-atom catalyst. Adapted from ref. [45].

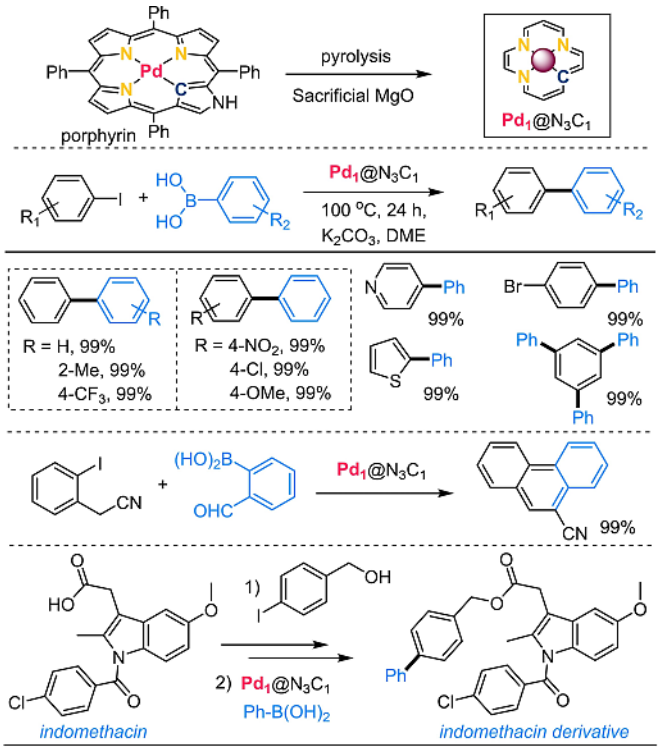

Scheme 14. Suzuki C–C coupling reaction catalyzed by a Pd single-atom catalyst. Adapted from ref. [47].

© 2023 The Authors. Angewandte Chemie International Edition published by Wiley-VCH GmbH

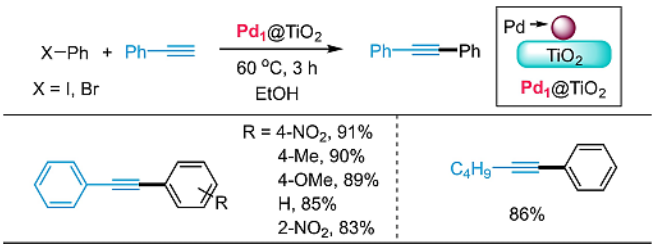

Scheme 15. Sonogashira C–C coupling reaction catalyzed by a Pd single-atom catalyst. Adapted from ref. [48].

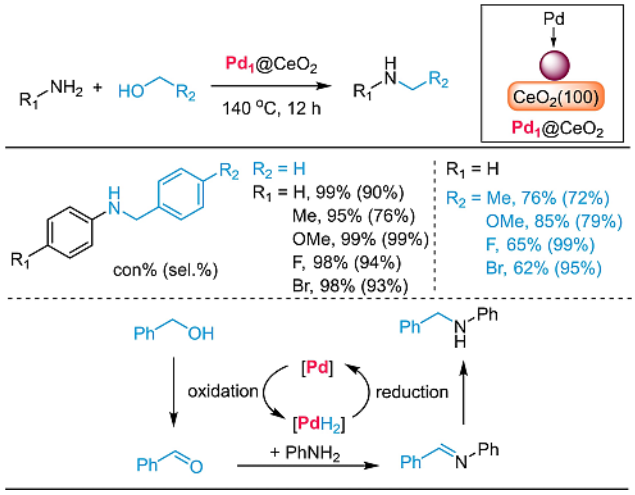

Scheme 16. Secondary amine synthesis from alcohols and primary amines over a Pd single-atom catalyst. Adapted from ref. [49].

nanoclusters were formed. The performance of the single-atom catalyst surpassed that of the material featuring nanoclusters for the alkylation reaction of primary amines with alcohols, yielding secondary amines as the final product. The proposed mechanism suggested the formation of a palladium hydride which was involved in the redox cycle.

An alternative development for the use of SACs in the cross coupling field was proposed by Ren et al., that developed Cu SACs featuring Cu–N_2 sites on N-doped porous carbon (derived from biomass), and used the system for Glaser-Hay coupling, another acetylenic homocoupling often catalyzed with copper (Scheme 17).[50] A wide range of terminal alkynes underwent homo- and hetero-coupling, affording 1,3-diynes with high efficiency.

Zhang et al. developed a similar Cu-based material, synthesizing a single-atom catalyst made of Cu species on N-doped graphene, featuring Cu–N_4 coordination sites. The material was obtained by pyrolysis of graphene in the presence of a copper salt (Scheme 18).[51] This catalyst was used for a C–N coupling reaction of alkylamines with aryl iodides, demonstrating the very broad applicability window of these materials in synthetic applications. Various substituted aryl iodides coupled with 2,3,4-tetrahydroisoquinoline and other cyclic, secondary, and primary amines. Based on DFT calculations, a proposed reaction mechanism

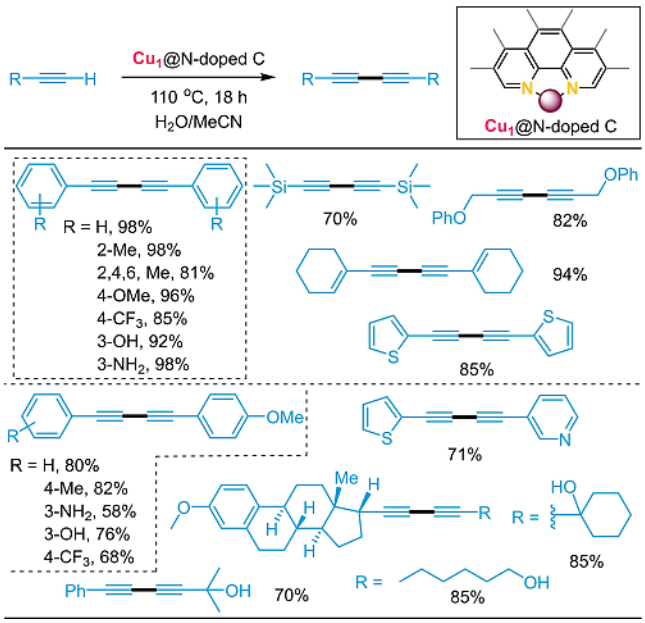

Scheme 17. Glaser–Hay homo-coupling of terminal alkynes catalyzed by a Cu single-atom catalyst. Adapted from ref. [50].

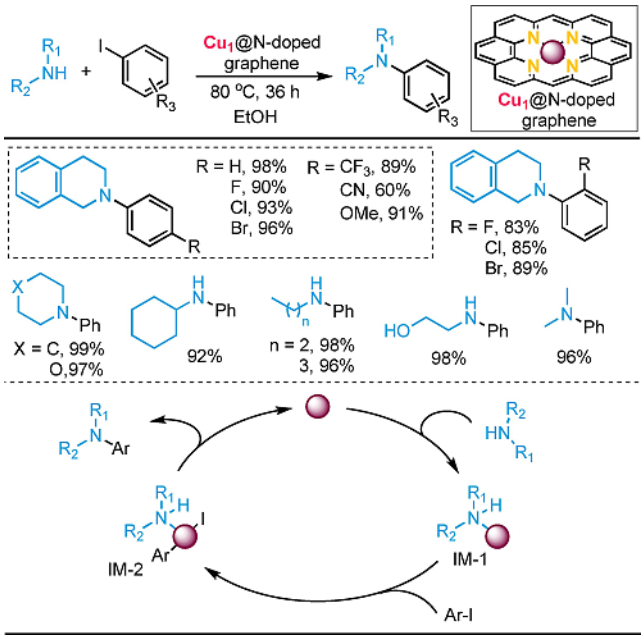

Scheme 18. C–N coupling reaction of alkylamines with aryl iodides carried out with a Cu single-atom catalyst. Adapted from ref. [51].

suggested that, on the catalyst surface, the amine binds on the copper atom and forms the intermediate-1 (IM-1), which undergoes oxidative addition with aryl iodide and leads to the intermediate-2 (IM-2). This subsequently undergoes reductive amination in the presence of a base to give the desired product.

Zhang et al. developed Co single atoms supported on mesoporous carbon by pyrolysis of cobalt-phenanthroline complexes (Scheme 19).[52] This catalyst was used to form

© 2023 The Authors. Angewandte Chemie International Edition published by Wiley-VCH GmbH

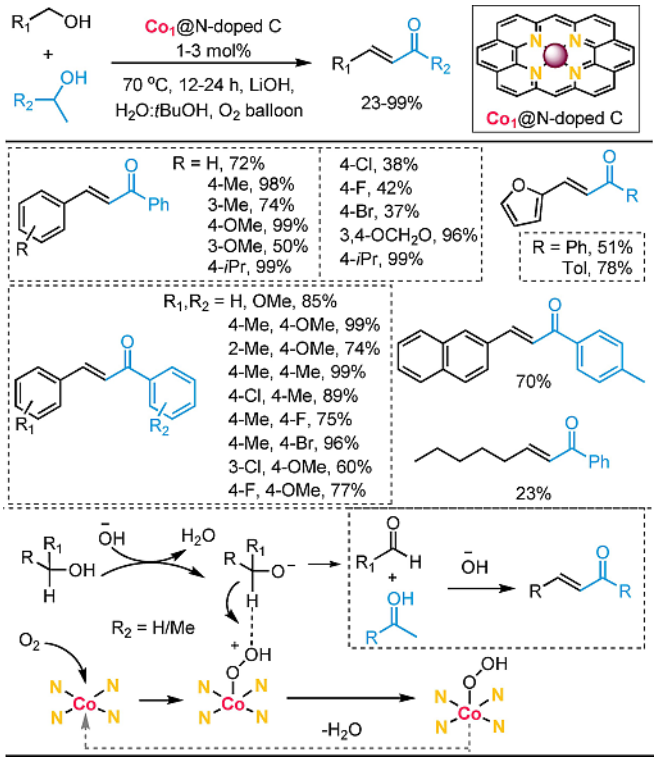

Scheme 19. α,β-unsaturated ketones synthesis from alcohols over a Co single-atom catalyst. Adapted from ref. [52].

C–C bonds via oxidative cross-coupling of primary and secondary alcohols to form α,β-unsaturated ketones. This catalyst tolerated various primary and secondary alcohols. A reaction mechanism was proposed based on experimental studies and theoretical reports, showing that the Co single atoms were the main active centers of the catalytic process to form carbonyl compounds.

Finally, Zhao et al. synthesized Ir single atoms anchored on a hollow carbon polyhedron material co-doped by N, P, and S atoms (Scheme 20).[53] This Ir single-atom catalyst was used for the carbene insertion of methyl phenyl diazoacetate with various alcohols, and led to an excellent TON (1456) compared to their homogeneous analogue (462). Along with alcohols, aniline and protected indole were also tolerated, and the catalyst showed excellent selectivity control (99 %), preferring benzylic O–H carbene insertion over phenolic O–H bonds. DFT calculations suggested that the electron-deficient coordination of the Ir carbene intermediate favored the benzylic O–H insertion. Despite the interest that this work has provoked, it is importat to highlight that iridium remains the least available metal on the earth. Thus, we believe that future research in the field of C–C cross coupling chemistry using SACs-based materials should focus on more earth-abundant metals.

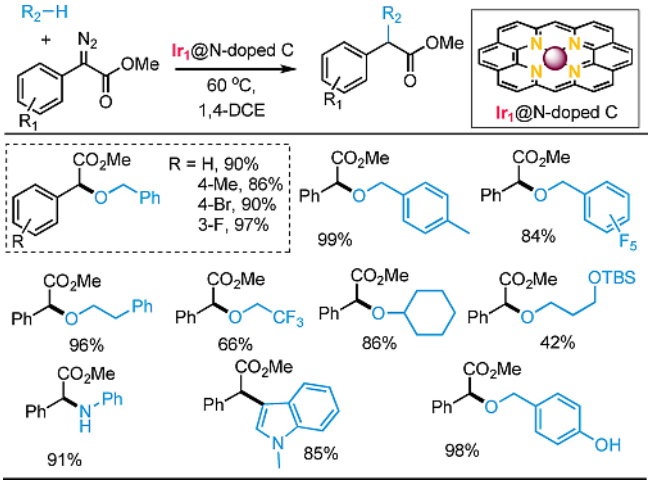

Scheme 20. Carbene insertion on methyl phenyl diazoacetate catalyzed by an Ir single-atom catalyst. Adapted from ref. [53].

3.3. Cycloadditions and click methods

Among the most exploited synthetic approaches, cyclizations and click methods are indispensable tools for synthesis. These reactions, which enable the construction of complex heterocyclic rings, are highly selective, requiring little or no downstream purification, and can be made from readily available starting reagents. Several reactions belong to this category, such as nucleophilic ring-opening reactions, non-aldol carbonyl chemistry, and cycloaddition reactions, especially 1,3-dipolar Cu-catalyzed Huisgen-type reactions. Most of these reactions are catalyzed using copper complexes; thus, this metal is also the most investigated for SACs-based studies. For example, Vilé et al. recently synthesized Cu SACs trapped inside a mesoporous gC_3N_4 material, and applied this for the three-component click reaction of azide, alkyne, and halide to give 1,2,3-triazoles under base-free conditions (Scheme 21).[54] These SACs were prepared by polymerization of tricyanomethanide to produce a joint electronic structure where the mesoporous graphitic carbon nitride ($mpgC_3N_4$) material acts as a multidentate ligand. The dispersion of copper species showed coordination of the metal with the heptazine pore of carbon nitride situated in a sandwich-like structure between the layers of $mpgC_3N_4$. This Cu catalyst offered an improved catalytic activity relative to homogeneous and heterogeneous analogues. A reaction mechanism was proposed based on DFT calculations, suggesting the initiation of the catalytic cycle via the adsorption of the acetylenic moiety on the Cu single atoms.

Another interesting application was developed by Chen et al., using a top-down pyrolysis method on natural wood to synthesize a porous carbonaceous support immobilizing single atoms of Fe, Co, Ni, and Cu.[55] Among them, Fe single atoms demonstrated a catalytic function for the one-pot synthesis of substituted quinolines by oxidative three-component cyclization of anilines, acetophenones, and DMSO, achieving 54–87 % isolated yields (Scheme 22). The

© 2023 The Authors. Angewandte Chemie International Edition published by Wiley-VCH GmbH

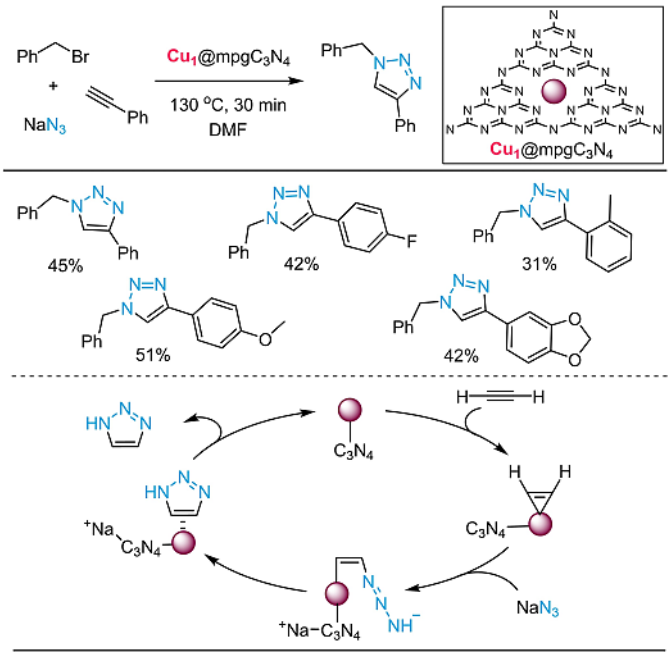

Scheme 21. Azide-alkyne 1,3-dipolar cycloaddition catalyzed by a Cu single-atom catalyst. Adapted from ref. [54].

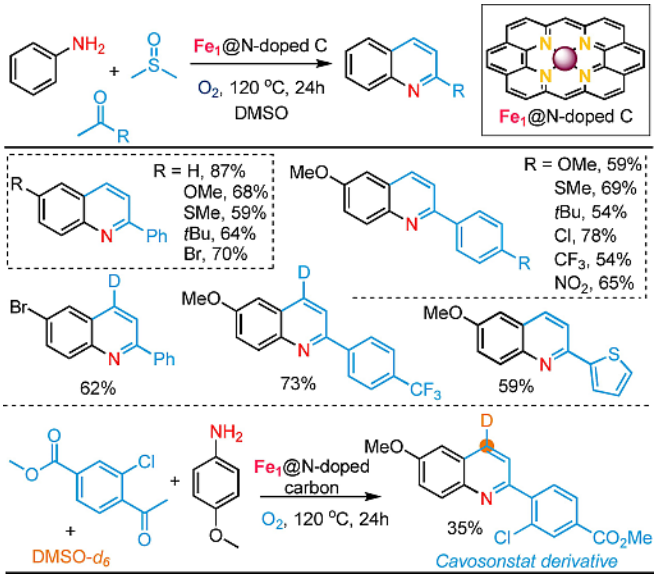

Scheme 22. Three-component quinoline derivative synthesis over a Fe single-atom catalyst. Adapted from ref. [55].

method was also applied to prepare cavosonstat, a novel, orally-bioavailable drug to treat cystic fibrosis.

3.4. Hydroelementations

Hydroelementations include a wide array of synthetic methods, featuring the insertion of E–H groups (with E = Si, B, Ge, P, Sn, N, O, *etc.*) on unsaturated C–C (both alkenes and alkynes) or C-heteroatom bonds (imines, nitriles, carbonyl compounds). The processes are primarily catalytic, and the stereo- and regioselectivity depend on the catalyst, reagent, and reaction conditions.[56],[57] Also in this case, the possibility to use SACs for this chemistry is not fully developed and only limited applications currently exist. However, it is possible to appreciate that, in most cases, single-atom catalysts based on expensive transition metals (e.g., on Pt and Au) are preferred.

Zhu et al. synthesized a Pt single-atom catalyst from pyrolysis of an EDTA-Pt complex and sacrificial Na_2CO_3 powder at 850 °C to obtain N-doped graphene supported with Pt single atoms.[58] This catalyst was used for the hydrosilylation of various terminal alkenes with anti-Markovnikov selectivity, producing tertiary silanes with an overall TOF of up to 180 h^{-1} (Scheme 23). This TOF was 4-fold higher than the benchmark Karstedt-type catalyst.

Liu et al. synthesized electron-deficient Pt single atoms supported on a carbonaceous material derived from artificial humic acid and urea, via a mild condensation and pyrolysis method (Scheme 24).[59] With this catalyst, the hydrosilylation of alkenes gave (at 70 °C for 1 min) TOFs up to 3×10^7 h^{-1}. DFT calculations suggested that the electron deficiency at the Pt center and the atomic dispersion of the metal sites were responsible for the increased catalysis. This result was similar to the work of Chen et al., who prepared partially charged Pt single atoms anchored on anatase TiO_2 ($Pt_1^{\delta+}/TiO_2$) and used them for the hydrosilylation of alkenes.[60]

Another class of relevant hydroelementation reactions is represented by hydroborations. These useful reactions allow for the attainment of boronic derivatives, i.e., boronic esters, often exploited as intermediates for further reactions (such as for the Suzuki coupling). Also for this class of reactions, selective reactivity has been demonstrated. Zhang et al. prepared nickel hydroxide ($Ni(OH)_x$) nanoparticles with several defects sites where the Ni atom was missing (i.e., vacancy of cationic Ni^{II}). The vacancies were used to stabilize Pt single atoms, with a Pt loading of up to 2.3 wt.%

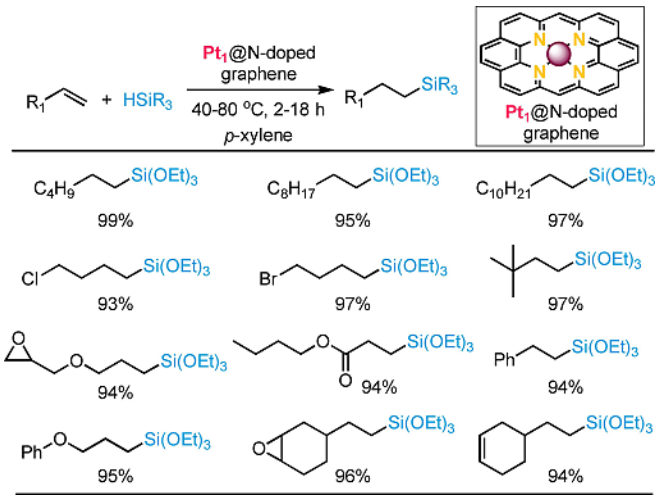

Scheme 23. Hydrosilylation of alkenes over a Pt single-atom catalyst. Adapted from ref. [58].

© 2023 The Authors. Angewandte Chemie International Edition published by Wiley-VCH GmbH

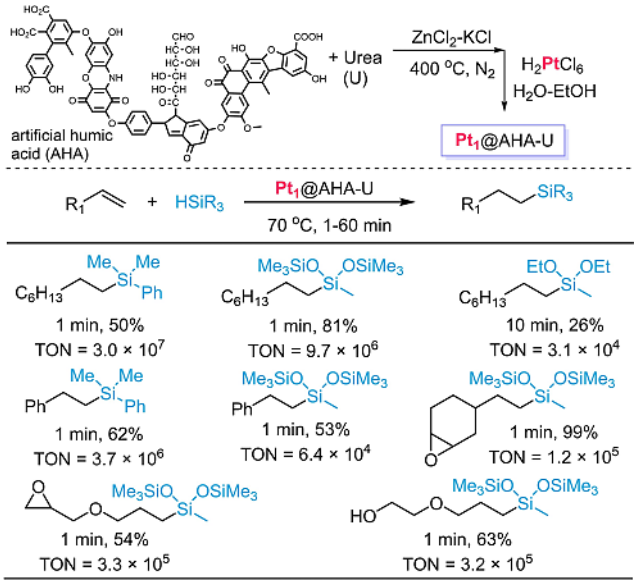

Scheme 24. Hydrosilylation of alkenes performed with a Pt single-atom catalyst. Adapted from ref. [59].

(Scheme 25).[23] This catalyst demonstrated excellent catalytic activity for the diboration of alkynes and alkenes, and an overall TOF of $\approx 3000\ h^{-1}$ was achieved. A reaction mechanism has been proposed, which suggests that the presence of vacancy sites in $Ni(OH)_x$ not only stabilizes the Pt atoms, but also assists in the breaking of the B–B bond in the diboron reagent due to the low coordination of oxygen. Initially, diboron dissociates on the surface of Pt, followed by activation and relative insertion of the alkyne to generate an acetylenic bond. Finally, the insertion of another boron into the ethylenic bond affords the final product.

Still focusing on noble metals, Feng et al. synthesized graphitic carbon nitride doped with Au single atoms (Scheme 26).[61] The presence of coordinating nitrogen species in gC_3N_4 helped stabilize the Au^I single atoms very efficiently. A range of aromatic and aliphatic alkyne substrates underwent hydrosilylation selectively at the β-(*E*) position (>98 %), and the catalyst was stable for the whole experimental campaign, i.e. over five consecutive catalytic cycles. A reaction mechanism was also proposed based on DFT calculations, suggesting that initially, silane undergoes an oxidative addition with Au^I to generate a silyl-Au^{III}-hydride intermediate. This intermediate then coordinates with the alkyne and undergoes silylmetallation, to finally afford (via reductive elimination) the β-(*E*)-vinylsilanes.

The reaction above proceeded smoothly due to the use of terminal alkynes. However, hydrosilylating internal alkynes remains a challenge, even over molecular catalysts. In this context, Sarma et al. recently reported an exciting example of tandem isomerization-hydrosilylation of internal alkenes, using both Rh and Ru single atoms supported onto CeO_2, obtaining 99 % selectivity.[62] Follow-up studies to further optimize this methodology (now requiring >24 h and an excess of reagents) can modulate this synthetic protocol for more industrially relevant conditions.

A similar approach was proposed by Zhang et al., that synthesized two types of Cu single atoms supported on CeO_2 nanorods by coating a melamine-formaldehyde resin (Scheme 27).[63] The Cu single-atom catalyst, with ionic polarity, demonstrated excellent catalytic activity for the

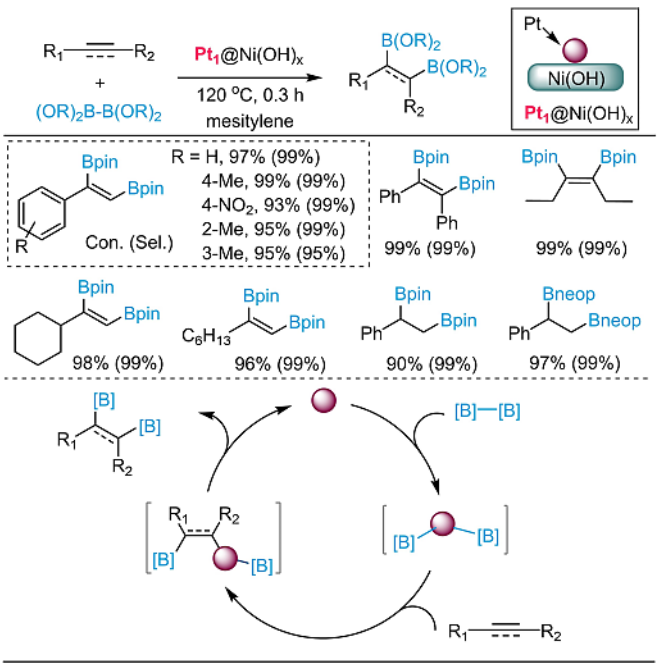

Scheme 25. Hydroboration of alkynes and alkenes over a Pt single-atom catalyst. Adapted from ref. [23].

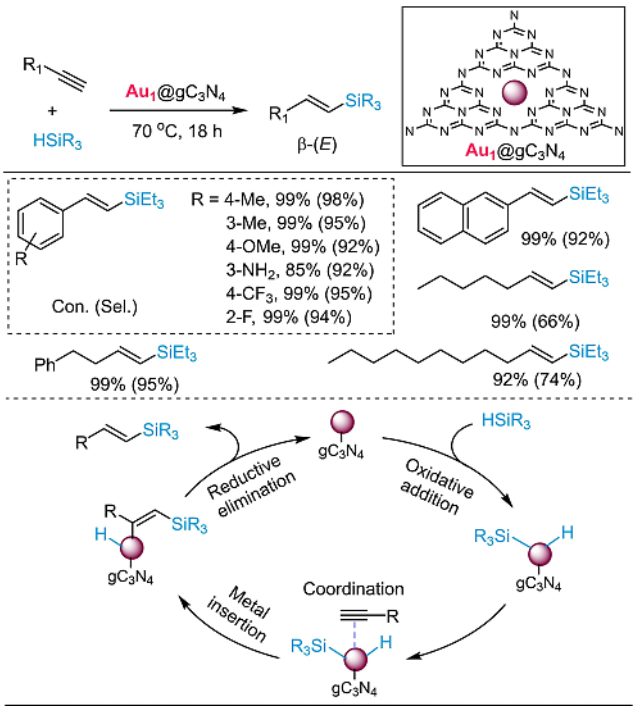

Scheme 26. Alkynes hydrosilylation catalyzed by an Au single-atom catalyst. Adapted from ref. [61].

© 2023 The Authors. Angewandte Chemie International Edition published by Wiley-VCH GmbH

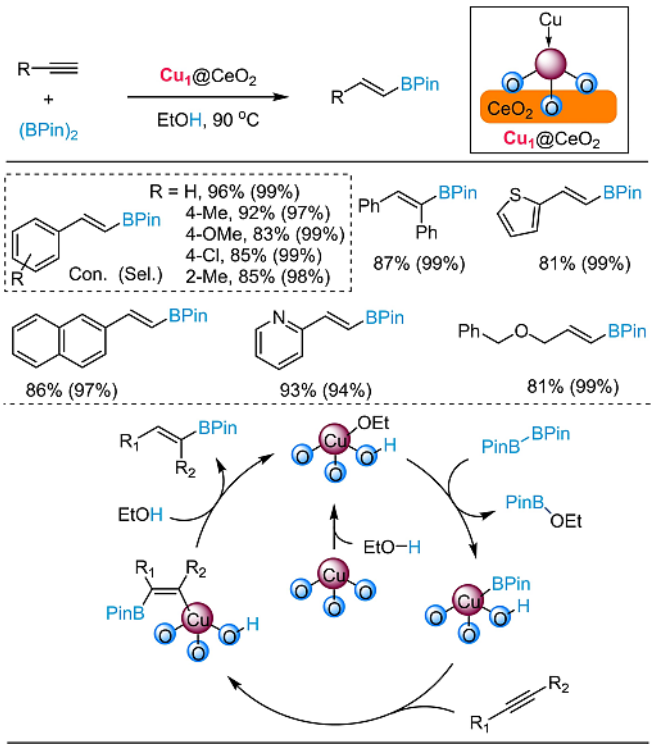

Scheme 27. Alkynes hydroboration over a Cu single-atom catalyst. Adapted from ref. [63].

hydroboration of alkynes to vinylboranes, compared with the Cu single-atom catalyst featuring more covalent Cu–O bonds.

In a follow-up study, Xu et al. exploited a defect engineering approach to dope magnesium (II) oxide (MgO) with Al^{III} species. This created vacant defect sites, which could anchor the Cu single atoms (Scheme 28).[64] This Cu single-atom catalyst demonstrated high stability and activity towards the hydrophosphonylation of alkenes to alkyl phosphorus structures, with anti-Markovnikov selectivity under mild reaction conditions.

Li et al. synthesized Cu atoms anchored on TiC, a transition metal carbide (TMC) support (Scheme 29).[65] This catalyst was used for the regioselective hydroboration of electronically different alkynes to linear species. A wide range of terminal alkynes were hydroborated very efficiently using B_2Pin_2, yielding a TON up to 600. Interestingly, a drug like cinacalcet hydrochloride was synthesized using a single-atom catalyst. The excellent recyclability of the sample, for up to eight consecutive reaction runs, demonstrated outstanding catalyst stability.

Finally, Tang et al. showcased an example of a single-atom catalyst for the C–N bond formation between alkenes and hydroxylamine (Scheme 30).[66] The catalyst allowed for aziridines and oxyamination products to be obtained in 25–60 % isolated yields. The protocol was also tested in late-stage functionalization of complex alkenes, obtaining phar-

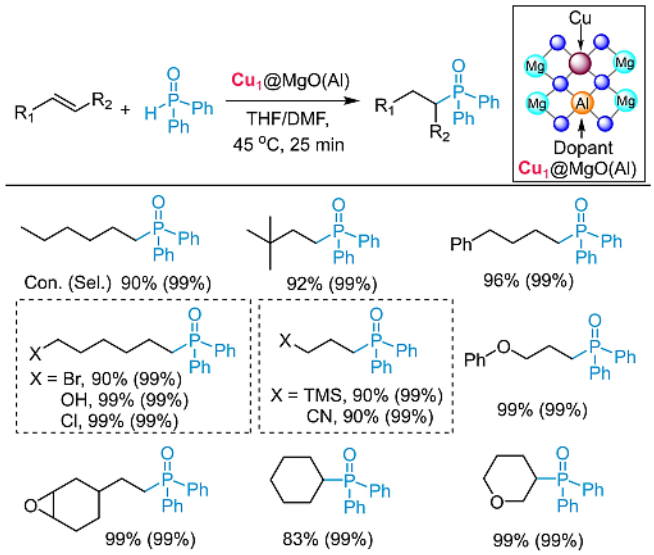

Scheme 28. Hydrophosphination of alkenes catalyzed by a Cu single-atom catalyst. Adapted from ref. [64].

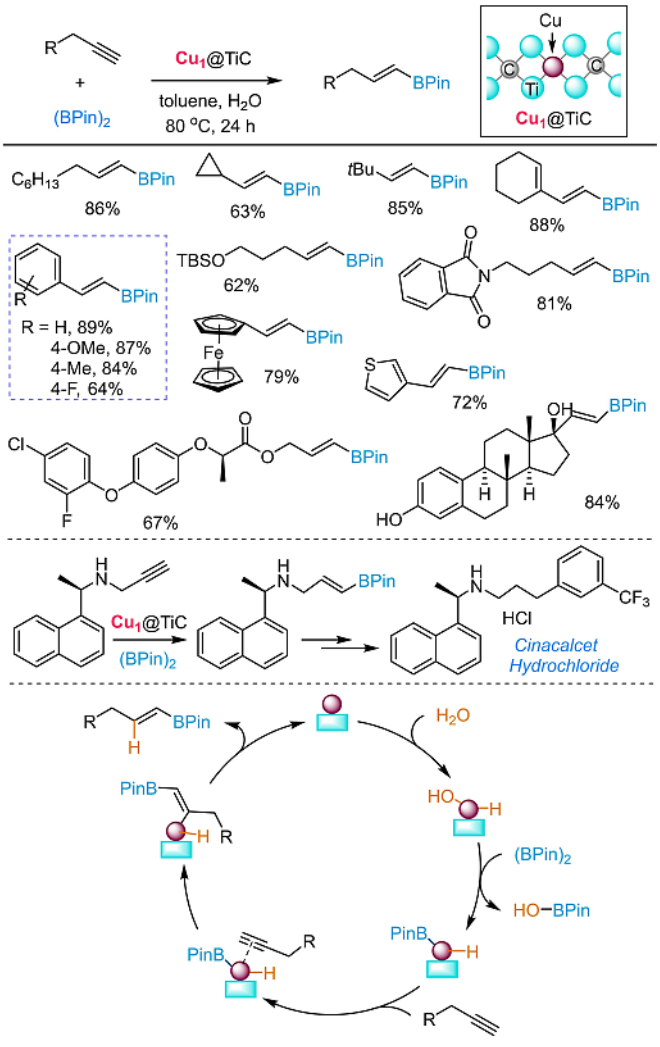

Scheme 29. Hydroboration of alkynes over a Cu single-atom catalyst. Adapted from ref. [65].

© 2023 The Authors. Angewandte Chemie International Edition published by Wiley-VCH GmbH

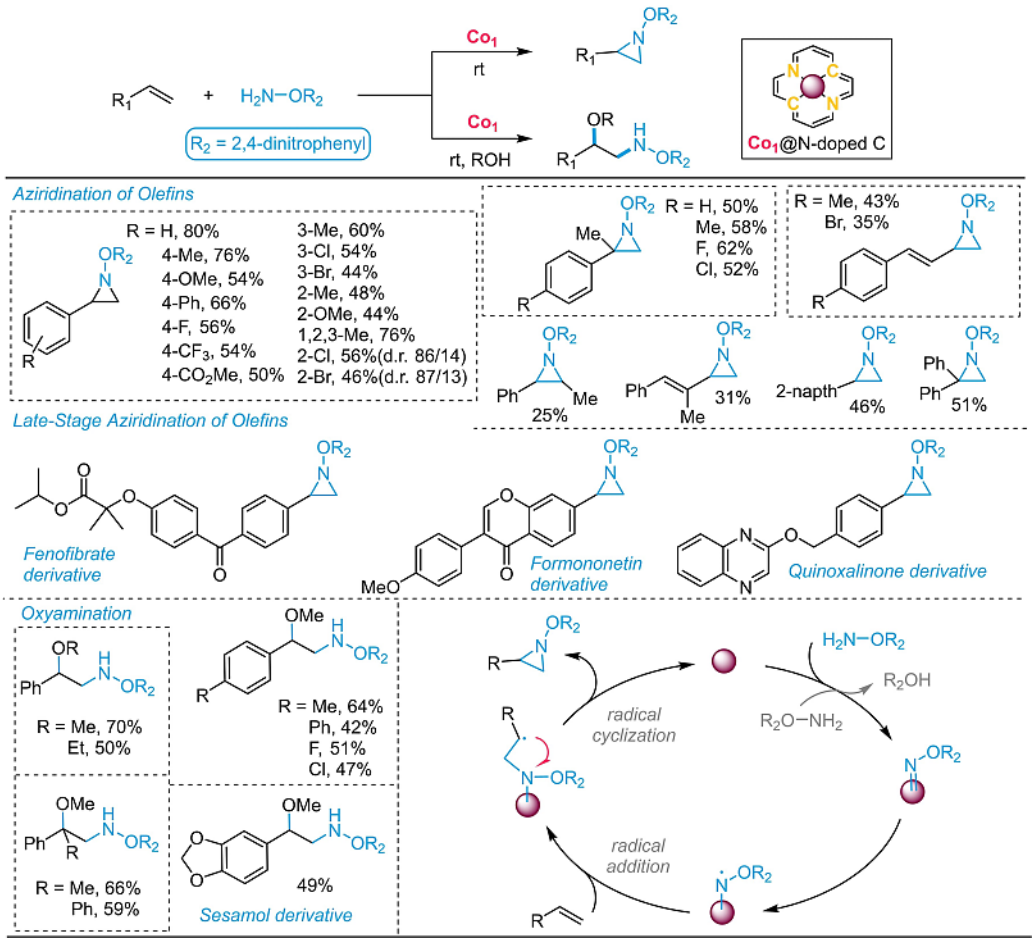

Scheme 30. Aziridination and oxyamination of olefins over a Co single-atom catalyst. Adapted from ref. [66].

maceutically useful derivatives from common scaffolds, like coumarin, fenofibrate, and tyroxine. Mechanistic studies revealed that $RONH_2$ species acted as a dual oxidant and nitrogen transfer reagent, which formed a cobalt imido intermediate with the Co_1@N/C catalyst. The triplet species was then generated, followed by the radical addition of alkene to the intermediate, affording the carbon radical species, which underwent radical cyclization to release aziridine and regenerate the catalyst. Finally, recyclability and gram-scale experiments revealed the flexibility and stability of the synthetic protocol (over seven reaction cycles).

3.5. Hydrogenations and reductions

Hydrogenations of unsaturated functional groups lead to the formation of saturated products by adding molecular hydrogen or using hydride donors (i.e., $LiAlH_4$, $NaBH_4$, $NaCNBH_3$, NH_3BH_3). A catalyst (often Pt, Ni, Co, and Pd-based materials) is typically needed to activate the reducing agent. In this context, several SACs have been recently reported for chemo- and regioselective hydrogenations.[67]

An early work by Vilé et al. showed the preparation of a Pd single-atom catalyst supported on mesoporous carbon nitride for the continuous-flow hydrogenation of alkenes and nitroarenes. The catalyst surpassed the activity of benchmark heterogeneous catalysts (i.e., Pd-HHDMA@TiS, Pd–Pb@$CaCO_3$, Pd@Al_2O_3), maintaining a very high degree of product selectivity (>90 %) for several hours on stream. DFT calculations elucidated that the high activity and selectivity was due to the enhanced hydrogen activation and alkyne adsorption on the atomically dispersed Pd sites. In this case, the N-rich support simultaneously acts as a spacer (distributing the active sites almost homogeneously), and as a ligand, promoting hydrogen activation.[68] A crucial aspect in hydrogenation chemistry with SACs is played by the support, and the activation mode of H_2 over the single-metal site, two aspects that are strongly interconnected. Indeed, different to metal nanoparticle-based catalysts, where the dissociation follows a homolytic pathway, in SACs the metal coordination environment can lead to both a homolytic or heterolytic activation of H_2, depending on the support used. As an example, the use of Pd_1@mpgC_3N_4 led to heterolytic activation, with one hydrogen bonded to Pd, and the other one bonded to the N atoms of the support;[68] on the other hand, Zhou et al. demonstrated the homolytic activation of

© 2023 The Authors. Angewandte Chemie International Edition published by Wiley-VCH GmbH

H_2 on the Pt single-atom site of a $Pt@WO_x$ $(2<x<3)$ catalyst.[69]

The reactivity of Pd SACs towards hydrogenation reactions has been extensively studied by others as well, corroborating the results in the previous work. Chen et al. anchored zero valent Pd atoms on a 2D black phosphorus material (Scheme 31).[70] This support typically comprises a high density of vacancy sites with low electronegativity, favoring Pd atom confinement. This catalyst was applied to selectively semi-hydrogenate various alkynes to alkenes using H_2 at 80 °C.

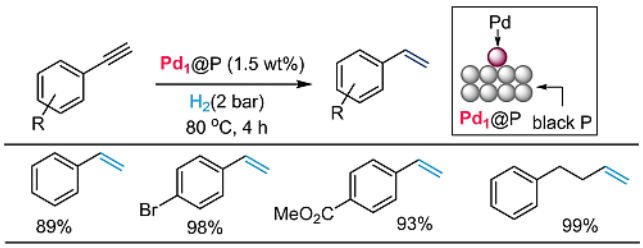

Scheme 31. Selective reduction of alkynes to alkenes over a Pd single-atom catalyst. Adapted from ref. [70].

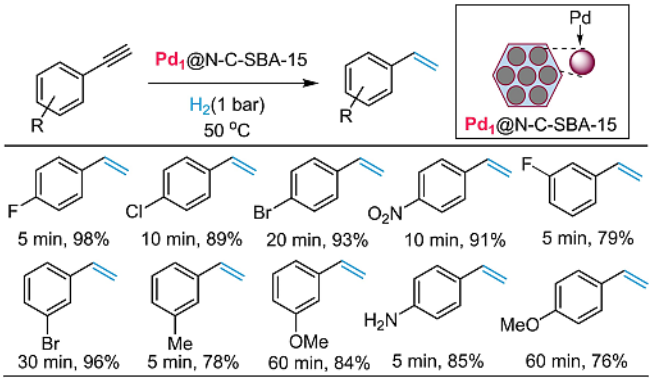

Scheme 32. Selective hydrogenation of alkynes to alkenes over a Pd single-atom catalyst. Adapted from ref. [71].

Li et al. synthesized a Pd single-atom catalyst, where metal atoms were anchored on nitrogen doped carbon shells over SBA-15 support, using a thermal atomization technique (Scheme 32).[71] This catalyst was efficient for the selective semi-hydrogenation of various alkynes to alkenes. A wide range of alkynes substituted with halides and electron withdrawing and donating substrates were tolerated efficiently, and the catalyst was also stable for six consecutive runs.

A completely different synthetic approach was used by Ji et al. In this case, the authors synthesized a catalyst where metalloporphyrins were co-polymerized with diluents, and subsequently pyrolysed to achieve an N-doped porous carbon material (Scheme 33).[72] On this carrier, Pt sites were immobilized. The obtained Pt single-atom catalyst displayed superior chemo- and regioselectivity for the hydrogenation of terminal alkynes, without affecting the other functional groups like internal alkynes, nitro, and terminal alkenes, with a TOF up to 5000 h^{-1}. The catalyst exhibited recyclability for up to five cycles without loss of its activity, and no formation of nanoparticles was observed.

Another development of the SACs contribution for hydrogenation reactions is represented by the work of Zheng et al., who used Al_2O_3 doping to decrease the N coordination number of the N-doped carbon material, achieved by pyrolysis of melamine-formaldehyde resin, and immobilized Cu single atoms.[73] Compared to the Al_2O_3-free Cu single-atom material, $Cu_1@$N-doped C–Al_2O_3 demonstrated a higher activity and excellent selectivity for transfer semi-hydrogenation of alkynes to alkenes with 84–98 % isolated yields (Scheme 34).

Most of the organic transformations catalyzed by SACs are investigated using common organic solvents, while the use of an aqueous media is rarely explored. Very recently, Liu et al. synthesized a hydrophobic Pd SAC on a sulfur doped carbon support ($Pd_1@$S-doped C). In this material, Pd single atoms were coordinated by sulfur, and the catalyst was used to perform semihydrogenation of alkynes to alkenes in water (Scheme 35).[74] The catalyst showed excellent reactivity and selectivity towards the alkenes, ca.

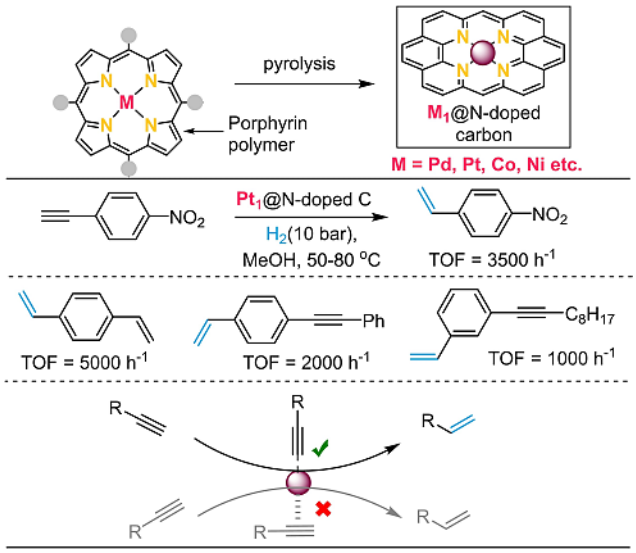

Scheme 33. Selective hydrogenation of terminal alkynes catalyzed by a Pt single-atom catalyst. Adapted from ref. [72].

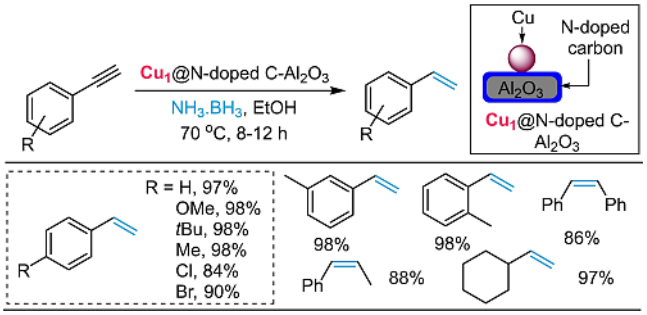

Scheme 34. Reduction of alkynes to alkenes catalyzed by a Cu single-atom catalyst. Adapted from ref. [73].

© 2023 The Authors. Angewandte Chemie International Edition published by Wiley-VCH GmbH

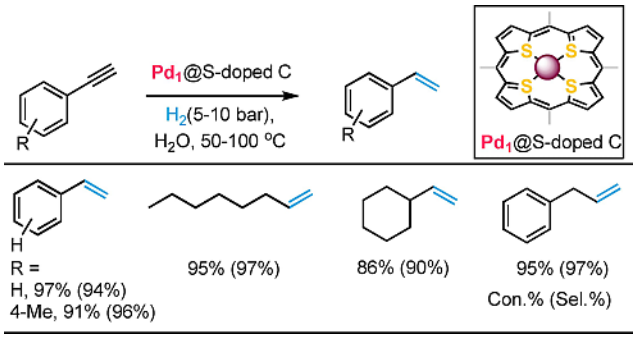

Scheme 35. Alkyne semihydrogenation catalyzed by a Pd-based single-atom catalyst. Adapted from ref. [74].

>90 % over alkane byproducts. In this case, the physical and chemical environments on the reaction interface behave quite differently, due to the employment of a hydrophobic support within an aqueous media. Indeed, contact angle measurements disclosed that the surface of Pd_1–S–C had a faster wetting rate of alkyne than the Pd_1–N–C catalyst, increasing reactant diffusion on a liquid-solid interface. Also, S-coordination of the Pd SAC promoted the interaction of the catalyst with the alkyne, as confirmed using adsorption capacity tests. Mechanistic calculations suggested that Pd single atoms in the PdS_4-containing catalyst are closer to the metallic state, in comparison with PdN_4-based materials; thus, the metallic state valency allowed for the achievement of a stronger H_2 chemisorption, enhancing the catalytic activity.

Peng et al. synthesized Pt isolated sites entrapped on the surface of nickel nanocrystals, and used the sample for the selective hydrogenation of nitroarenes (Scheme 36).[75] A chemoselective synthesis of the aniline product was achieved with a TOF of ≈1800 h^{-1}, higher than other Pt nanoparticles supported on nickel, active carbon, TiO_2, silica, and zeolite carriers.

A similar Pt-based SAC on an inorganic support was studied by Ye et al. The authors synthesized a stable Pt single-atom catalyst confined in the sub-nanometer cavities of $CaO \cdot Al_2O_3$. They used the catalyst for the chemoselective hydrogenation of nitroarenes to the corresponding anilines, reaching TOFs up to 25×10^3 h^{-1} (Scheme 37).[76]

A completely different composite support was reported by Chen et al. The authors synthesized a Pt single-atom catalyst on a MoS_2/graphite felt flow stack, and used it for chemoselective reduction of nitroarenes to anilines under a fast-flow process. An excellent TOF ($>8 \times 10^3$ h^{-1}) and productivity (5.8 g h^{-1}) were achieved over a variety of functions, such as ketone, aldehyde, nitrile, ester, *etc.* (Scheme 38).[77]

Transition metal carbides exhibit excellent stability, ordered morphology, and a rich electronic environment, thus acting as an excellent support for the stabilization of metal single atoms. Recently, Ma et al. used vacancy-enriched molybdenum carbide (α-MoC) to stabilize Pd

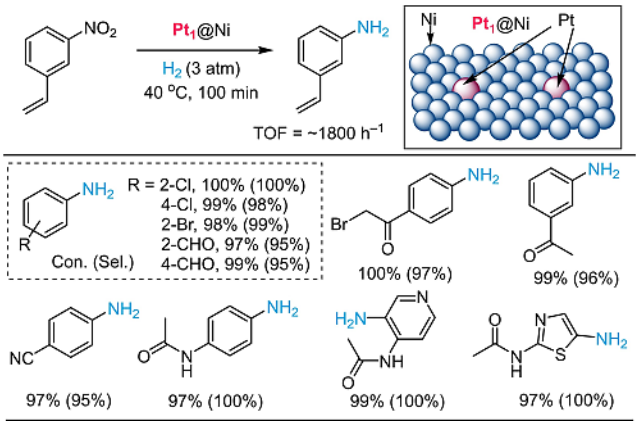

Scheme 36. Nitroarenes hydrogenation over a Pt single-atom catalyst. Adapted from ref. [75].

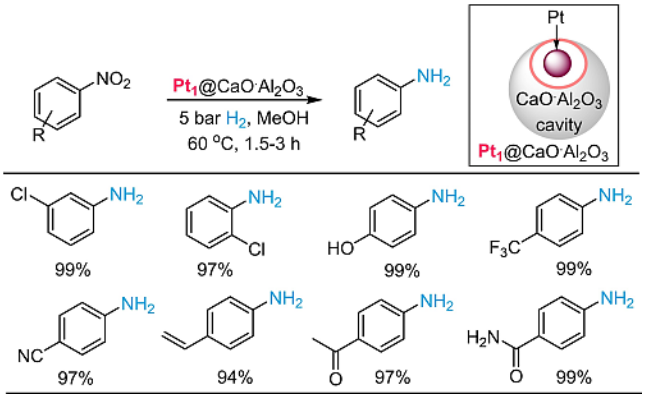

Scheme 37. Hydrogenation of nitroarenes catalyzed by a Pt single-atom catalyst. Adapted from ref. [76].

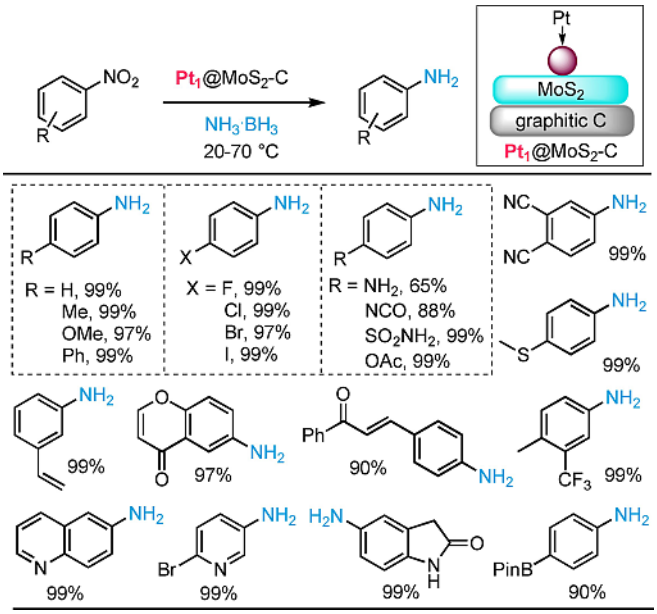

Scheme 38. Nitroarenes hydrogenation over a Pt single-atom catalyst. Adapted from ref. [77].

© 2023 The Authors. Angewandte Chemie International Edition published by Wiley-VCH GmbH

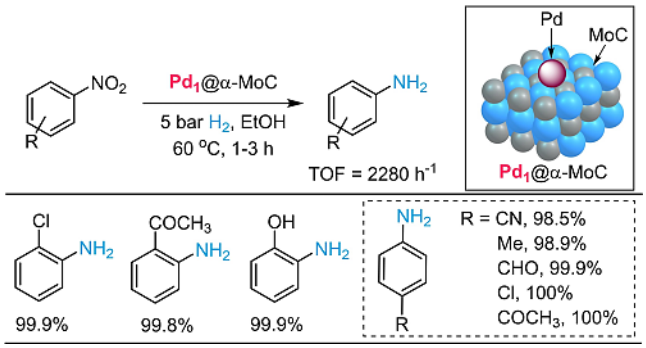

Scheme 39. Pd single-atom catalyst catalyzed hydrogenation of nitroarenes. Adapted from ref. [78].

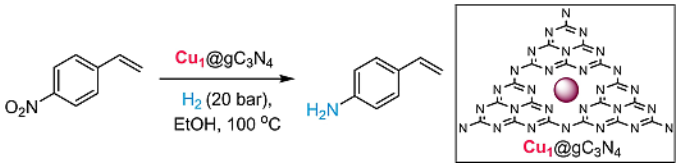

Scheme 40. Selective hydrogenation of nitroarenes to anilines catalyzed by a Cu single-atom catalyst. Adapted from ref. [79].

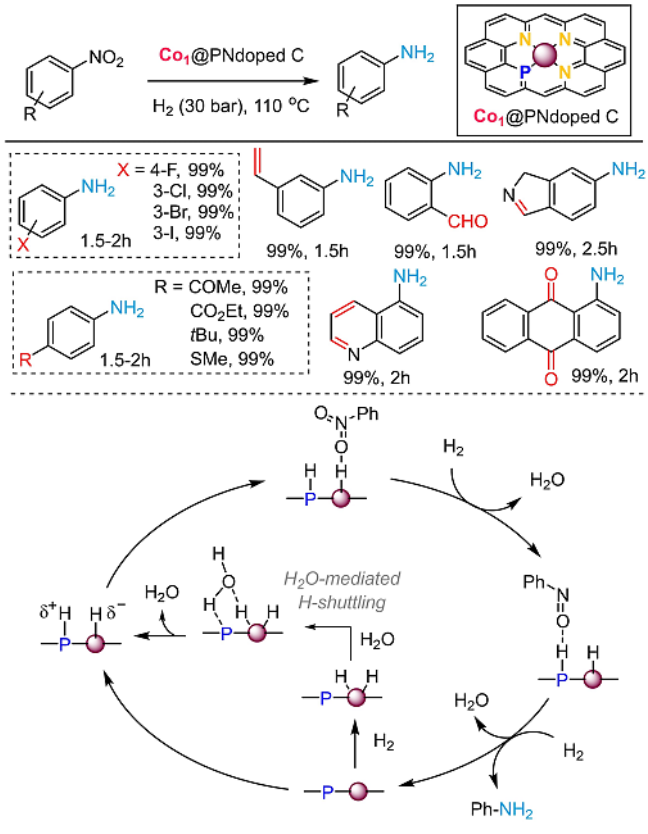

Scheme 41. Co single-atom catalyst catalyzed hydrogenation of nitroarenes. Adapted from ref. [80].

single atoms (Scheme 39).[78] The Pd isolated sites exhibited strong interaction with α-MoC support and offered high loading of Pd (5 wt.%). The catalyst was used for the selective hydrogenation of substituted nitroarenes to anilines and CO_2 hydrogenation.

Chen et al. demonstrated that graphitic carbon nitride is an excellent support for stabilizing SACs.[32] Inspired by this, Liu et al. synthesized atomically-dispersed Cu single atoms on the melem ring of gC_3N_4 (Scheme 40).[79] This catalyst had exceptional stability, high selectivity (100%), and excellent activity (TOF = 2.9×10^3 h^{-1}) for the hydrogenation of 4-nitrostyrene to 4-aminostyrene.

Electronic and geometric properties of the support play an important role for stabilizing SACs. Jin et al. recently designed a Co SAC using an asymmetrical coordination mode, where phophorous was doped along with nitrogen (N_3) (Scheme 41).[80] In this case, the presence of the P atom increased the electron density around the Co single atom in the Co_1–N_3–P_1 motif, compared to the Co_1–N_4 equivalent. This catalyst was used for the hydrogenation of several functionalized nitroarenes to the corresponding anilines. A high TOF (6560 h^{-1}) was obtained, which was approximately 60-fold higher than the Co_1–N_4 variant. Moreover, this SAC offered optimal chemoselectivity (>99%) for substituted nitroarenes. This catalyst had high stability and showed recyclability for up to five cycles. A slight decrease in the yield was observed, and was ascribed to the loss of catalyst. Mechanistic studies suggest that the H_2 molecule initially cleaves heterolytically at the Co_1–N_3–P_1 site, with the assistance of the H_2O-mediated H-shuttling mechanism, which correspondingly generates Co–$H^{\delta-}$ and P–$H^{\delta+}$.

Long et al. synthesized a graphitic phosphorous support and used the sample to stabilize Fe single atoms (Fe_1@gP).[81] This catalyst was used to conduct reductive amination reactions (Scheme 42). In a similar approach, Liu et al. synthesized Pt single atoms supported on defect-rich CeO_2 nanorods, and used the material for the selective synthesis

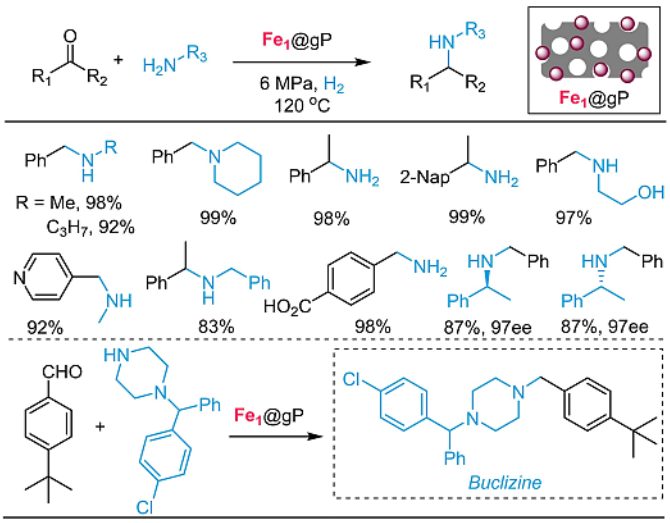

Scheme 42. Reductive amination catalyzed by a Fe-based single-atom catalyst. Adapted from ref. [81].

© 2023 The Authors. Angewandte Chemie International Edition published by Wiley-VCH GmbH

of *E*-hydrazone esters from α-diazoesters, using NH_3BH_3 as the reducing agent (Scheme 43).[82] The Pt single atoms accelerated the alcoholysis of NH_3BH_3 from readily-available carboxylic esters compared to nanoparticle-based Pt catalysts, giving an isolated yield for the *E*-hydrazones within the range of 56–89 %, and an overall TOF $>500\ h^{-1}$. Interestingly, the method was also extrapolated to prepare various 1*H*-indazole-based pharmaceutical scaffolds and ^{15}N-labeled analogs, such as gamendazole, granisetron, and nigellicine. A reaction mechanism was proposed where, in the presence of Pt, the alcoholysis of amine borane complex with methanol is adsorbed on the surface of cerium oxide, generating a hydride. Then, the α-diazoester adsorbate coordinates with the Pt center, and hydrogen transfer from the hydride occurs. Finally, another hydride molecule shifts to afford *E*-hydrazone as a final product, with the regeneration of the catalyst for the next cycle.

Differently from the works discussed herein, Zhang et al. used an innovative template sacrificial strategy for synthesizing Co, Fe, Ni, and Cu single atoms immobilized on various mesoporous silica materials (i.e., MCM-41, SBA-15, and FDU-12).[83] Among them, Co atoms on SBA-15 presented excellent catalytic activity for the hydrodeoxygenation of lignin-derived scaffolds like vanillin, and hydrogenation of nitroarenes to anilines (Scheme 44).

Exploiting defect engineering, Liu et al. synthesized Pd atoms supported onto defect-rich nanodiamond graphene (n-graphene), and used the solid powder for the selective transfer hydrogenation of nitriles to secondary amines, using amine borane as a reducing agent (Scheme 45).[84] Various nitriles underwent transfer hydrogenation efficiently and gave excellent turnover frequencies (above $700\ h^{-1}$) and selectivity (>98 %) to the secondary amines. DFT calculations revealed that the single atom follows a dissociative adsorption pathway of H_2. The hydrogenation route then involves the generation of the benzylideneimine intermediate, which leads to secondary amines.

Vilé et al. successfully merged single-atom catalysis and reactor design, to conduct a flow hydrogenation reaction. The authors designed a 3D-printed, structured flow reactor, and integrated it with a thin layer of Cu single atoms supported on the mesoporous gC_3N_4 material, for use in the continuous-flow hydrogenation of benzaldehyde and furfural to the corresponding alcohols.[85] The fabricated catalytic reactor configuration was highly efficient and allowed for

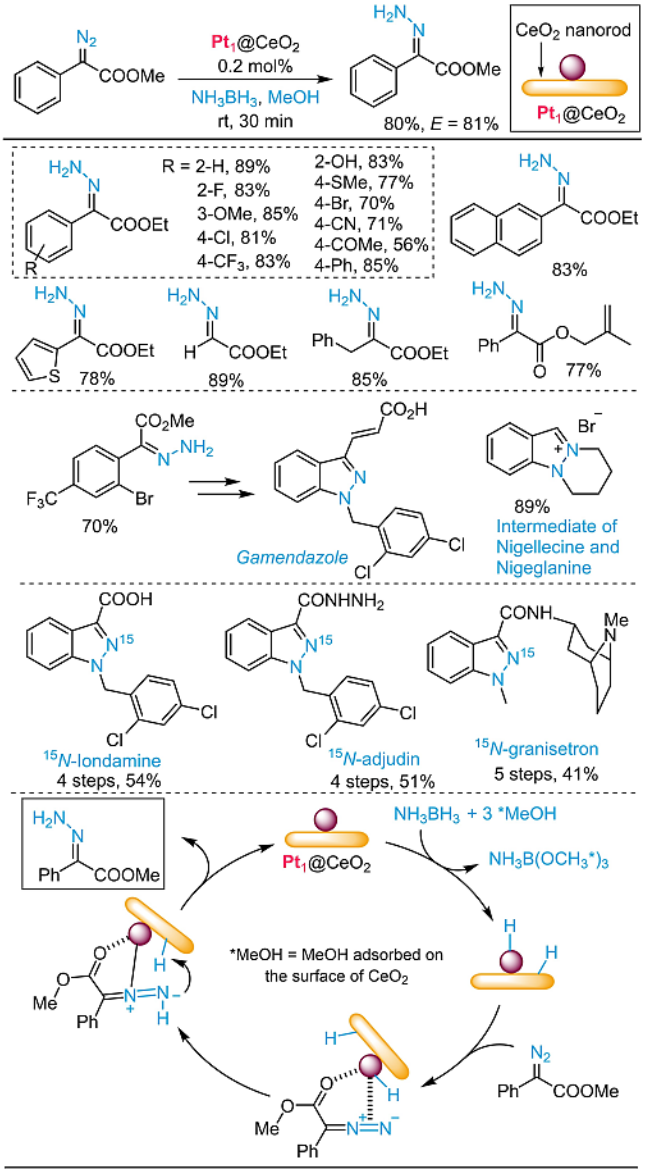

Scheme 43. Synthesis of unprotected *E*-hydrazone esters from α-diazoesters catalyzed by a Pt single-atom catalyst. Adapted from ref. [82].

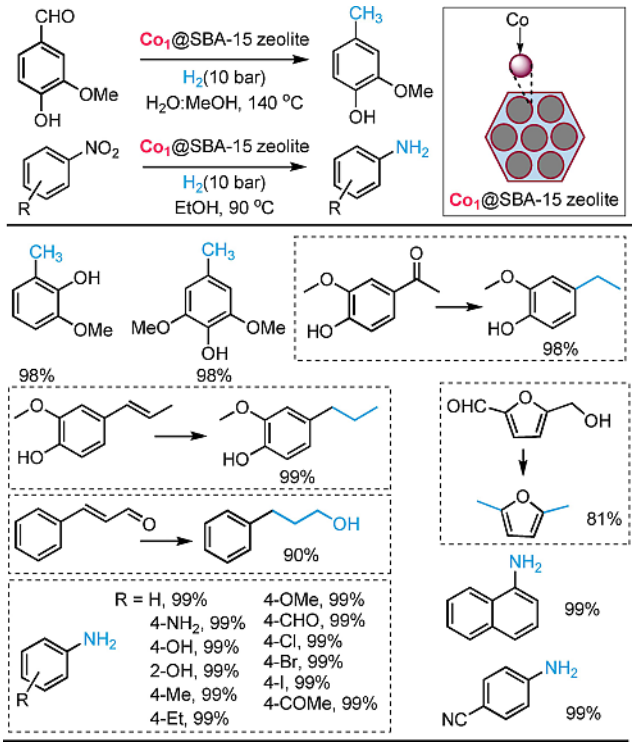

Scheme 44. Hydrogenation of aromatic aldehydes and nitroarenes over a Co single-atom catalyst. Adapted from ref. [83].

© 2023 The Authors. Angewandte Chemie International Edition published by Wiley-VCH GmbH

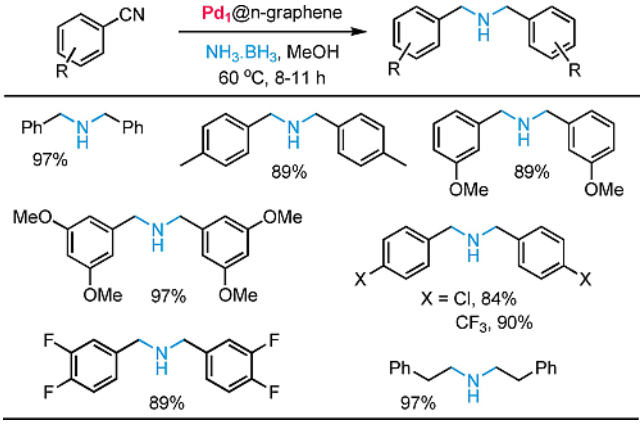

Scheme 45. Reduction of nitrile to amines catalyzed by a Pd single-atom catalyst. Adapted from ref. [84].

optimal results to be obtained in the hydrogenation of aromatic aldehydes.

Focusing on the utilization of SACs for a tandem hydrogenation-cyclization reaction, Gao et al. synthesized a Co single-atom catalyst using the in situ generated cobalt-phenanthroline complexes on a carbon support, via impregnation and pyrolysis, followed by acid treatment.[86] This catalyst was used for the reductive amination of levulinic acid (Scheme 46). The same catalyst also showed relevant catalytic activity for the in situ synthesis of amines by hydrogenating nitro- and nitrile functional groups, with 65–97 % isolated yields (Scheme 47). The approach was also extended to the industrial synthesis of indoprofen, an important drug with anti-inflammatory, analgesic, and antipyretic properties.

Focusing on a different aspect, Li et al. demonstrated that a defect engineering strategy could be used to anchor Pd single atoms on the oxygen defects of CeO_2 nanorods (Scheme 48). This Pd single-atom catalyst was used for the selective hydrogenation of styrene (TOF = 2400 h^{-1}), the chemoselective hydrogenation of cinnamaldehyde (TOF = 968 h^{-1}), and the oxidation of triethoxysilane (TOF = 10000 h^{-1}).[87] The material showed high selectivity and stability, and was reused for up to five cycles while preserving the dispersion of Pd single atoms on the support. Similarly, a good selectivity towards the hydrogenation of conjugated double bonds was observed by Li et al. using Pd sites stabilized on defective β-FeOOH nanorods. The same authors later investigated the selective hydrogenation of cinnamaldehyde to hydrocinnamaldehyde on the same catalyst, reporting TOFs up to 2450 h^{-1} and selectivities up to 99 %.[88]

3.6. Hydroformylations

Hydroformylation reactions yield aldehydes, using olefins and syngas (CO/H_2O) as starting materials. Traditionally, this reaction class was conducted using Co and Rh-based metal catalysts. Rh is the most used metal in the case of

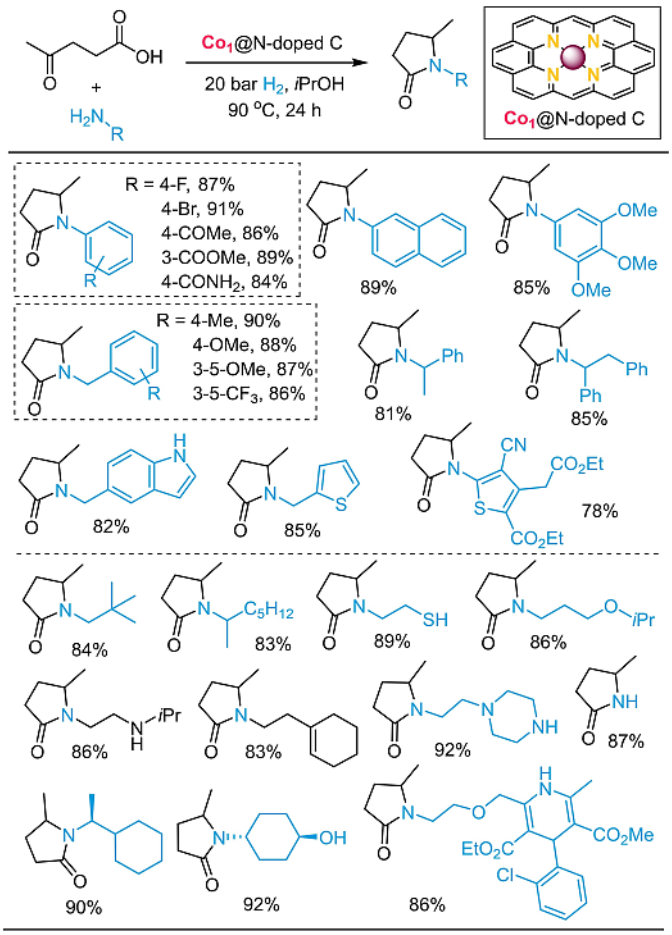

Scheme 46. Reductive amination of levulinic acid over a Co single-atom catalyst. Adapted from ref. [86].

SAC-based hydroformylations. For example, Rui et al. exploited Rh on ZnO for the formylation of olefins,[89] while Li et al.[90] and Amsler et al.[91] reported Rh ionic species anchored onto CeO_2 for the hydroformylation of styrene (Scheme 49).

Similarly, Gao et al. used a nanodiamond (C) support connected with phosphorus amine (PNP) coordinated ligands in order to stabilize the same active phase made of Rh single atoms (Scheme 50).[92] Excellent regioselectivities towards branched aldehydes were obtained. The catalyst was also used for the gram-scale synthesis of several drugs, such as ibuprofen and fendiline.

3.7. Carboxylation and fluorination

Catalytic fixation of carbon dioxide (CO_2) to value-added chemicals is crucial for effectively utilizing CO_2 as a starting reagent. These types of reactions are typically performed using Pd-based catalysts. Nevertheless, the only existing applications with SACs are based on earth-abundant elements. In this regard, Yang et al. used mesoporous carbon nitride to stabilize Cu single atoms at extremely high loading (26.6 wt.%) and utilized the catalyst for the carbon-

© 2023 The Authors. Angewandte Chemie International Edition published by Wiley-VCH GmbH

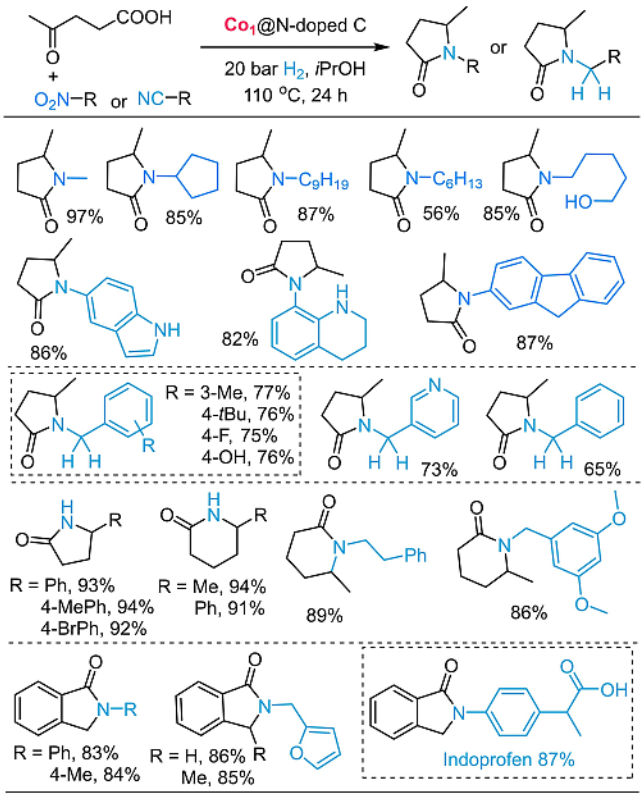

Scheme 47. In situ synthesis of amines using a Co single-atom catalyst. Adapted from ref. [86].

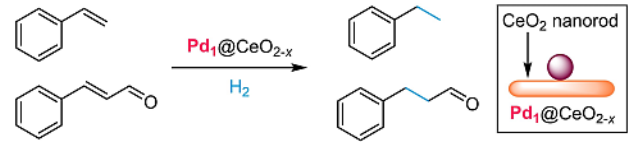

Scheme 48. Pd single-atom catalyst catalyzed hydrogenation of alkenes. Adapted from ref. [87].

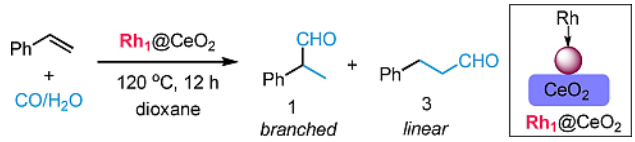

Scheme 49. Hydroformylation of alkenes performed with a Rh single-atom catalyst. Adapted from ref. [90, 91].

ylation of terminal alkynes (Scheme 51).[93] Various substituted phenyl acetylenes and heterocyclic alkynes were tolerated (60–97 % isolated yields). The catalyst was recyclable for several runs, but the absence of any metal aggregation (given the intrinsic loading of metals) was not unambiguously proven.

Another crucial reaction for organic and pharmaceutical synthesis is represented by fluorination protocols, vis-à-vis the introduction of fluorine atoms on aromatic and aliphatic skeletons. Due to the importance of this reaction, and of the resultant fluorinated products, several efforts have been made to improve the reaction rate, also involving the use of SACs for such an enhancement. From this perspective, Li et al. investigated the use of a Co-based single-atom catalyst for the fluorination of acyl chlorides (Scheme 52).[94] The protocol showed good catalytic performances with variously substituted aromatic and aliphatic acyl chlorides. The TON achieved, 1.58×10^6, was 16000 times higher than benchmark literature values. The high substrate compatibility demonstrated by the catalytic system also allowed the modification of various complex acyl chlorides, which are key intermediates in the production of pesticides like tebufenpyrad and tolfenpyrad.

4. Light-driven organic synthesis using SACs

Recently, as an alternative to conventional (thermal) methods, light-driven processes are gaining increasing attention as a way to utilize clean and sustainable energy sources in order to catalyze chemical reactions.[95] Most practiced and studied photoredox catalysts are based on homogeneous transition metal complexes comprising moisture-sensitive ligands and critical elements (e.g., Ir or Ru).[96] Hence, impressive efforts are being made towards the design of active, selective, and durable heterogeneous photoredox catalysts containing only earth-abundant elements.[97] In the case of heterogeneous platforms, the metal and the support play two different but interconnected roles. The support must therefore be photoactive, and produce excited state charges in the presence of visible light irradiation. These can in-turn oxidize or reduce the single metal sites, which partake in their own catalytic cycle with the reagent (organic) molecules.[98] In this sense, the choice of both the support and the metal are crucial points to address in designing a SAC-based metallaphotoredox system.

He et al. synthesized Pt sites supported on gC_3N_4, and used the catalyst for the chemoselective hydrogenation of nitroarenes to anilines under visible light irradiation.[99] On the other hand, Cui et al. synthesized a single-atom catalyst containing Ag^+ ions supported on $Mg(OH)_2$ (Scheme 53).[100] Under visible light irradiation, this catalyst underwent reductive borylation of aryl iodides to aryl and vinyl boronates with a TOF of $1.4 \times 10^4\ h^{-1}$ under very mild conditions.

Recently, Niu et al. used CdS as a photoactive support for stabilizing Pd sites. The composite was exploited for light-derived *N*-alkylation of amines using alcohols by a hydrogen transfer process (Scheme 54).[101] The surface of CdS helps to stabilize the Pd SACs through the Pd–S_x species. Mechanistic investigations suggested that, in the presence of visible light, Pd_1@CdS helps to efficiently generate and trap electrons, increasing the lifetime of the photoexcited state.

Differently from the previous cases, Wang et al. synthesized Co single atoms on carbon quantum dots (CDs), featuring Co–N_4 anchoring sites.[102] Under visible-light conditions, the catalyst was used for the oxidative imine formation from alcohol and amine, leading to high con-

© 2023 The Authors. Angewandte Chemie International Edition published by Wiley-VCH GmbH

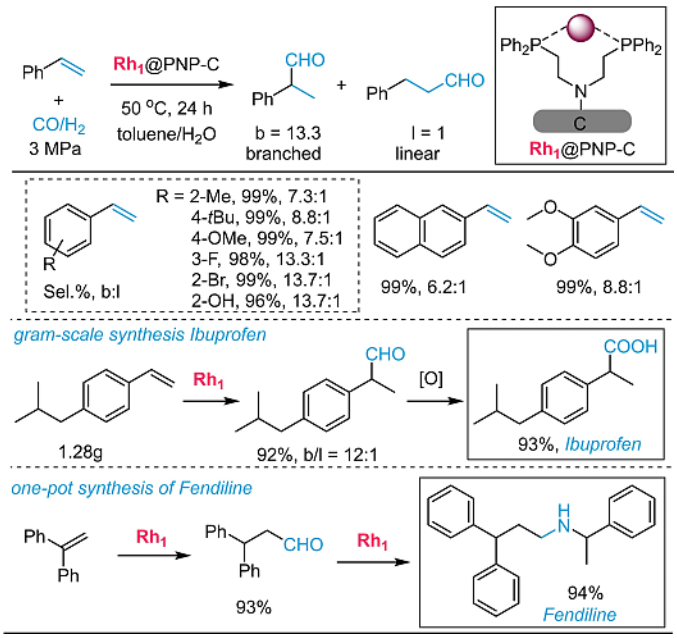

Scheme 50. Hydroformylation of alkenes over a Rh single-atom catalyst. Adapted from ref. [92].

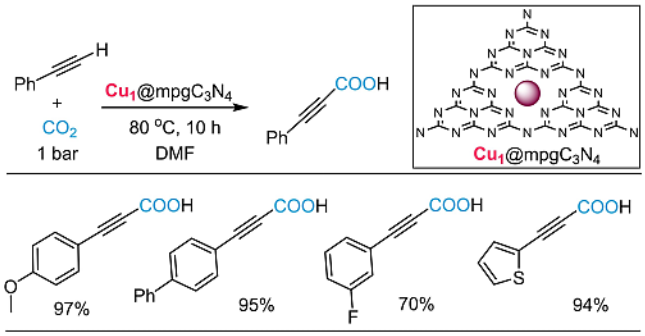

Scheme 51. Carbonylation of alkynes over a Cu single-atom catalyst. Adapted from ref. [93].

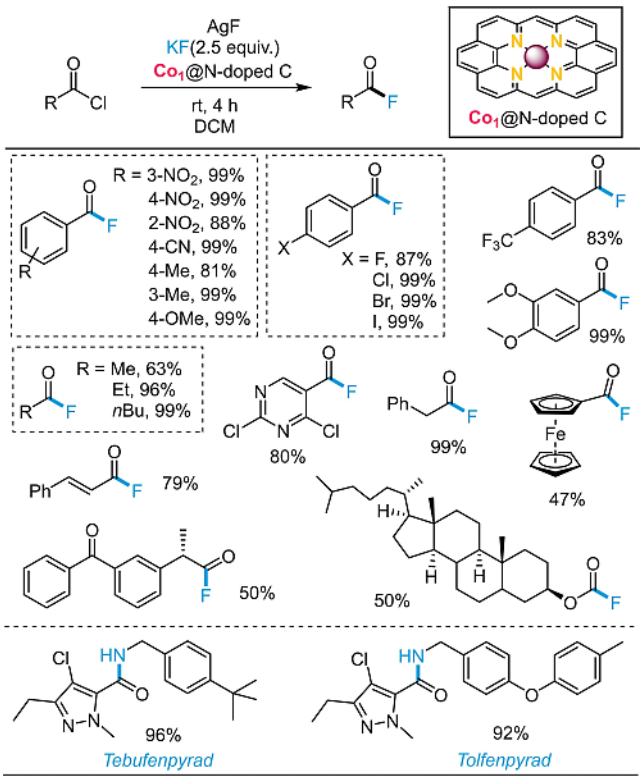

Scheme 52. Fluorination of acyl chlorides over a Co single-atom catalyst. Adapted from ref. [94].

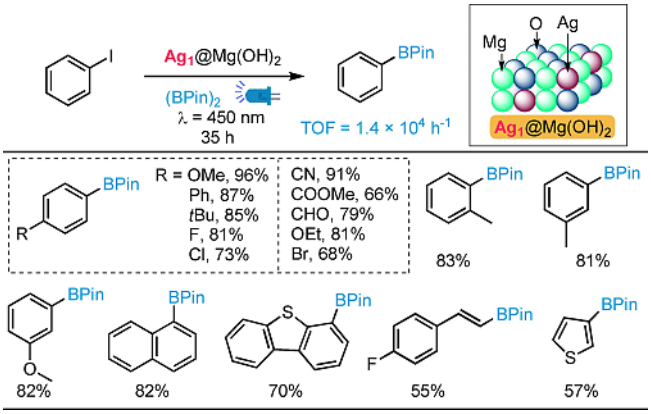

Scheme 53. Borylation of aryl iodides catalyzed by a Ag single-atom catalyst. Adapted from ref. [100].

version (~ 90 %), and imine selectivity (> 99 %). In a similar fashion, Ma et al. exploited the peculiar reactivity of Ni single atom supported on carbon nitride for imine photocatalyzed synthesis starting from benzyl alcohol and several amines (Scheme 55).[103] DFT calculations suggested that the Ni single atoms assist the adsorption and activation of the substrates to generate highly-reactive oxygen species, which are responsible for the catalytic cycle.

Kwak et al. investigated the use of Ni single atom supported on graphitic carbon nitride for the photocatalyzed C–N coupling of alkyl amines and aryl halides, in presence of visible light. (Scheme 56).[104] The catalytic reactions proceeds smoothly with both primary and secondary amines, as well as with aryl iodides, chlorides, and bromides. Mechanistic studies suggested that the photoactive C_3N_4 support is useful to activate the Ni species on the catalyst via electron transfer; simultaneously, the photogenerated holes are quenched by pyrrolidine, which forms a pyrrolidine radical. Thus, Ni^0 species is generated under light irradiation, and oxidative addition of aryl halides to Ni^0 produced the Ni^{II} intermediate, that coordinates pyrrolidine radical to produce the Ni^{III} species. Finally, the reductive elimination of Ni^{III} intermediate afforded the desired product, leading to catalyst regeneration.

© 2023 The Authors. Angewandte Chemie International Edition published by Wiley-VCH GmbH

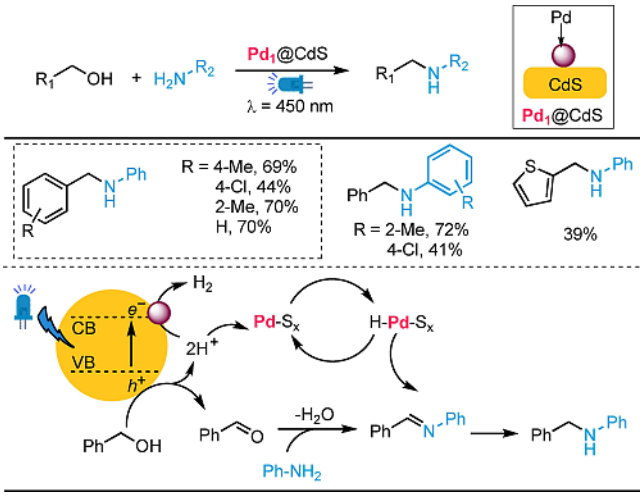

Scheme 54. Photocatalyzed *N*-alkylation of amines over a Pd single-atom catalyst. Adapted from ref. [101].

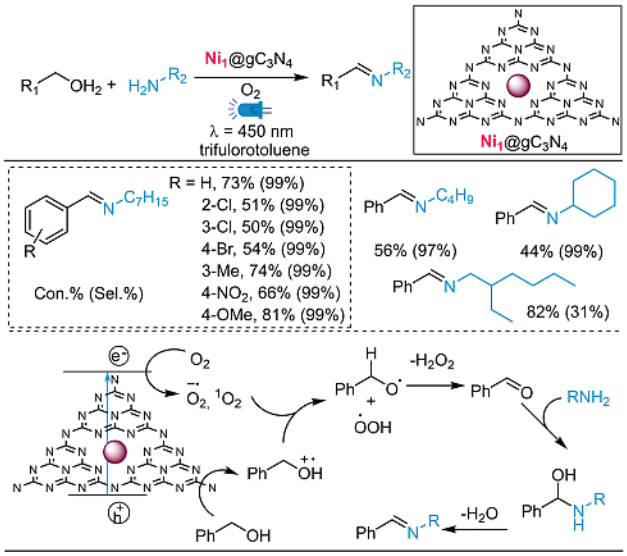

Scheme 55. Oxidative imine formation photocatalyzed by a Ni single-atom catalyst. Adapted from ref. [103].

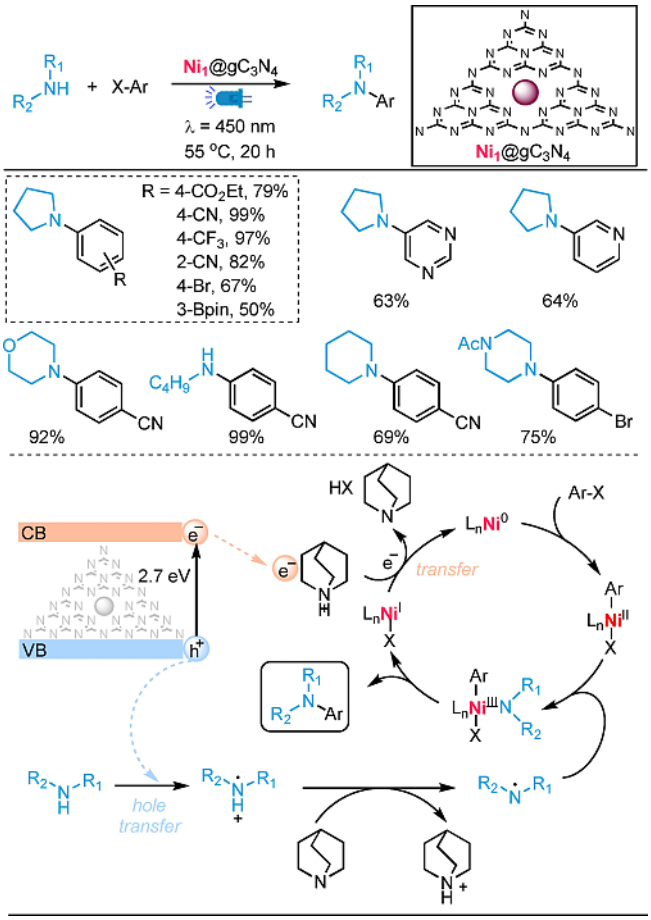

Scheme 56. C–N coupling photocatalyzed by a Ni single-atom catalyst. Adapted from ref. [104].

5. Designing SACs for organic synthesis: a "helicopter" overview

5.1. Metal selection

The previous sections have presented some of the most exciting applications of SAC for organic sysnthesis, in which SACs have enhanced the system performance relative to more conventional catalytic approaches. However, the various catalytic systems (with different metals, carriers, and conditions) call for a more rational analysis. For this reason, we conducted an in-depth (data-driven) literature analysis, wherein a variety of reactions encountered above, and commonly utilized in synthetic, medicinal, and industrial applications, have been cross-referenced with the type of transition metals employed (see the Supporting Information file published online for the thorough breakdown of the individual search, and exemplary specific query strings used for the survey). This investigation has allowed us to determine which metals are in the highest demand for each synthetic case, which particular reactions are most studied and implemented, and which metals are being pursued on a single-atomic level (for each respective organic synthetic application described herein).

Based on Figure 2, from a classic catalytic standpoint (i.e., including both homogeneous and heterogeneous catalysts), palladium is the most common choice of catalyst for C–C coupling; nickel and iron presume the highest number of published works for hydrogenation and oxidation chemistry, respectively. Regarding SACs, platinum and palladium maintain the top positions among the most widely studied metals (despite a constant quest and need to optimize and reduce the quantity of precious metals). This is followed closely by iron, cobalt, copper, and nickel, indicative of recent trends in the catalysis sector to adopt more sustainable and earth-abundant metals to carry out the reactions our society relies on. The reaction class most examined with SACs is "oxidation", and here, all the metals have at least one related publication.

© 2023 The Authors. Angewandte Chemie International Edition published by Wiley-VCH GmbH

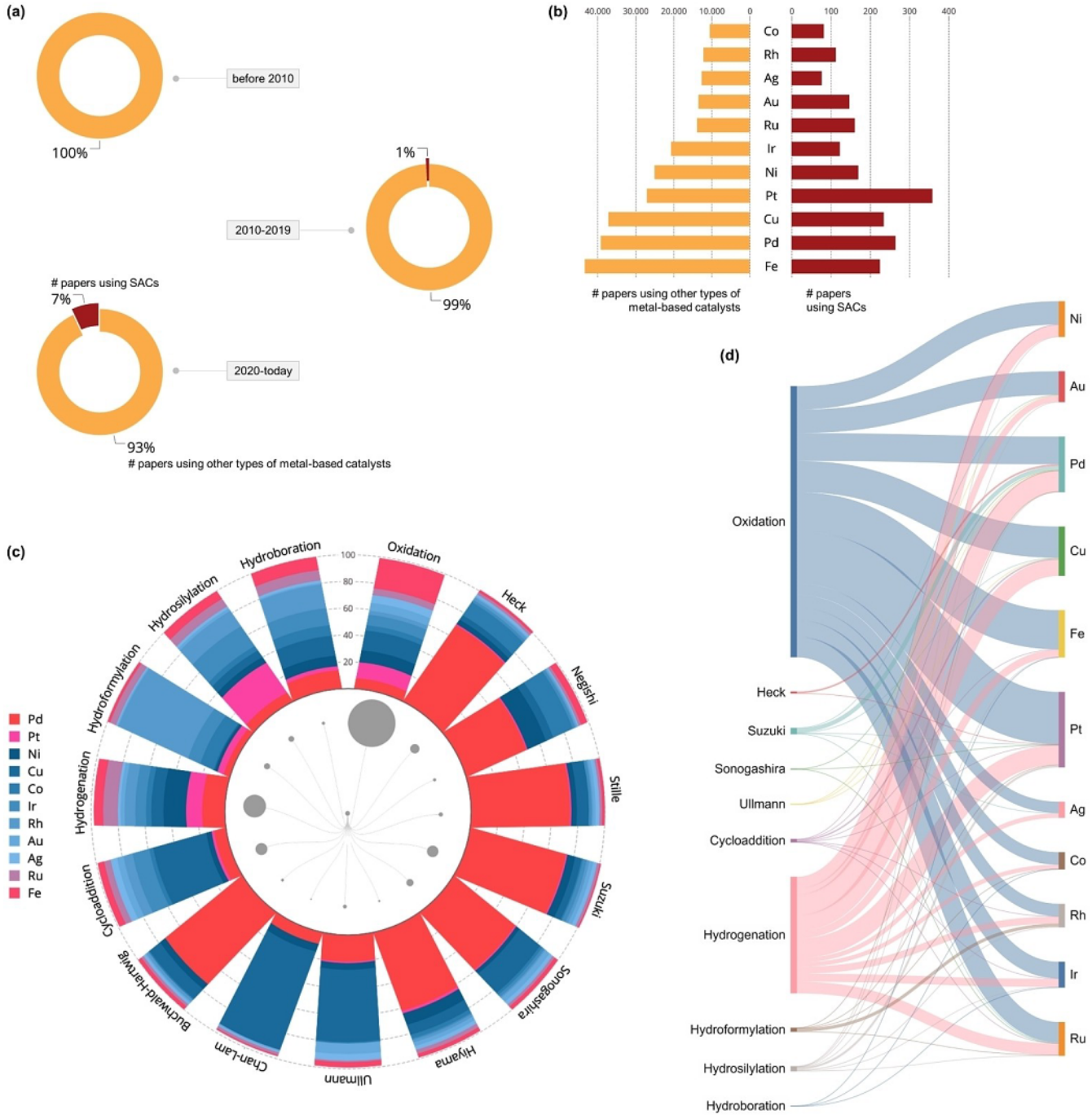

Figure 2. (a) Donut charts highlighting a growing trend in the use of SACs for organic synthesis. (b) Bar charts showing *vis-à-vis* the metals most used in synthetic chemistry over conventional catalysts (homogeneous and heterogeneous, denoted as "other type of metal-based catalysts" on the Figure) and SACs. (c) Polar bar chart focused on SACs-based organic transformations, depicting the type of metals most applied in each reaction. The circular dendrogram within the polar bar chart depicts the amount of papers for each reaction (larger diameters correspond to a higher fraction of papers), which highlights the relevance of each reaction in the literature. (d) Alluvial diagram correlating SACs-based organic reactions with active metals. The literature survey has been conducted using Scopus, searching the whole literature database and using the query strings included in the Supporting Information document published online.

5.2. Untapped reaction and metal opportunities

The findings also reveal the growth potential of the field of SACs, where numerous combinations of "metal SACs"-"reaction class" have not yet been analyzed systematically (denoted by the zero hits for a significant portion of catalyst-reaction varieties). This can offer scientists working in the fields of organic chemistry and catalysis novel avenues to explore, design, and tailor a diverse array of SACs for applications in several transformations. Figures 2 and 3 can

© 2023 The Authors. Angewandte Chemie International Edition published by Wiley-VCH GmbH

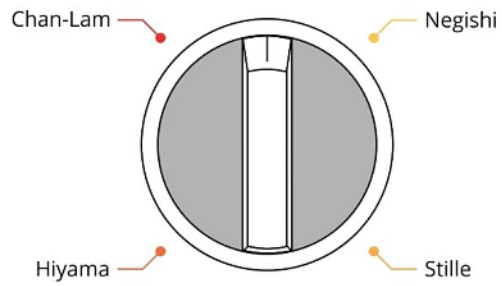

Figure 3. Organic reactions not yet developed using metal-based SACs.

thus serve as practical tools for researchers in associated fields to guide and direct them towards underexplored single-atom catalyzed reactions.

5.3. Chemical versatility and orthogonality

SACs are highly desirable because of their optimal atom utilization and structural similarity to ligand-coordinated organometallic catalysts. This has led to an interest in SAC-mediated liquid-phase organic transformations. As shown in the previous sections, several studies have demonstrated that SACs can achieve remarkable chemoselectivity in hydrogenations and oxidations, owing to a preferential interaction of the isolated metal site with specific functional groups. The application of SACs in important cross-coupling reactions, including Suzuki, Ullmann, Sonogashira, and Heck coupling, to construct C–C, C–O, and C–N bonds, have been reported. These reactions generally involve a dynamic change in the valence state of the catalytic center during the oxidative addition-reductive elimination pathway; however, achieving a delicate balance between structural flexibility and leach resistance in the catalyst design is possible.

One of the most important advantages of SACs is their chemical orthogonality (i.e., a combination of high stereo-, regio-, and chemoselectivity to specific transformations and functional groups).[102] Such orthogonality originates from the restricted adsorption configuration over a single metal in contrast to the multiple binding sites over conventional metal surfaces. This has also been corroborated by FTIR operando studies. For instance, $Pt_1@MoS_2$ prefers a monodentate "end-on" adsorption of the nitro functionality compared to the planar binding configuration of the alkene groups on Pt nanoparticles, which induces a chemoselectivity of 99 % toward 3-aminostyrene.[81]

5.4. Catalyst synthesis

From our literature survey, 79 % of all papers utilizing SACs in organic synthesis involve stabilizing metal species on a solid support through wet chemistry. This remains a common catalyst synthesis approach due to its simple operation and easy access to the appropriate raw materials. This method includes co-precipitation and impregnation, carried out with mild heat or at room temperature. Photoradiative or electrochemical deposition are also viable strategies for this approach.[13–15] The precursors employed in synthesizing SACs are organometallic complexes or inorganic salts. When the precursors are organometallic complexes, the as-prepared SACs are mainly formed with organic ligands. Once the ligands are removed, the SACs will aggregate together. The perspective by Hu et al.[106] provides a complete overview of how to make SACs in a conventional chemistry lab.

6. Conclusions and outlook

Synthetic organic chemistry is one of the most impactful areas of research in science. The marriage between SACs and organic chemistry has been elegantly demonstrated in the literature. Among the advantages, SACs can reduce the overall cost of the catalytic system, maintain sustainability through low metal atom utilization, and, in several cases, enhance the reaction efficiency. This review has described the progress in this field, focusing on thermal and photochemical reactions. We have shown that SACs based on Pd and Pt are widely explored for coupling, hydrogenation, and hydroelementation reactions. SACs comprised of Co, Cu, and Fe are repeatedly used, instead, in oxidation chemistry. We have also scanned the enormous number of publications and devised some guiding tools (in the form of easy-to-interpret graphical representations) to assist other researchers in the field of catalysis, for selecting appropriate "SACs-reaction" combinations. This is a novel (data-driven) approach for summarizing and capturing the key highlights, knowledge gaps, and possible research directions for pursuing SACs-based organic synthesis.

Although significant progress has been made, the development of SACs continues to encounter numerous challenges in their design:

1) *Coordination:* the stabilization and performance of SACs is critically dependent on the coordination environment of the metal, and even minor changes during synthesis can substantially affect the local structure, and consequently, the catalytic activity, selectivity, and stability. Therefore, it is crucial to synthesize SACs with a precisely defined coordination environment. However, achieving this remains a formidable challenge, primarily due to the difficulty in designing solid supports with a uniform and well-defined surface structure. Furthermore, it is worth noting that in certain instances, the synthetic methods employed have resulted in the formation of mixed systems consisting of both single atoms and nanoparticles.[107] In such cases, a synergistic catalytic mechanism may operate, emphasizing the need to determine the dissimilarities in atomic structures and electronic states of distinct metal species to elucidate their respective roles.
2) *Stability:* SACs may become unstable under harsh reaction conditions, leading to significant metal leaching in the presence of corrosive species in the reaction mixture. As a consequence, characterizing these catalysts under realistic reaction conditions, and obtaining accurate data on their structure and post-catalysis metal

© 2023 The Authors. Angewandte Chemie International Edition published by Wiley-VCH GmbH

loading, are essential aspects to bear in mind when comparing new single-atom systems with state-of-the-art analogues.

3) *Synthetic scalability and reproducibility:* the production of SACs on a large scale remains challenging due to the time-consuming nature of synthetic procedures and the requirement of expensive precursors or specialized and intricate instruments. Zhang et al. recently reported the successful scale-up of single-atom catalyst synthesis to a kilogram scale,[108] representing a significant step towards the industrial production and application of these catalysts. However, further research is still required to optimize the scalability of the synthesis process and ensure that the resulting SACs exhibit consistent performance and stability across different batches. Moreover, the low metal loadings of most SACs continue to restrict their applicability in a wide range of synthetic processes, which is attributed to the challenge of producing SACs with a high metal content.[109] Although a few studies have demonstrated the possibility of high metal loading in SACs,[110] the use of such systems in chemistry remains limited.
4) *Mechanistic understanding:* the incomplete understanding of the oxidation states and catalytic behavior of SACs poses obstacles to optimizing reaction conditions and rationally designing new materials. To elucidate such mechanisms, advanced in situ and operando characterization techniques may be required. However, this is not immediate because the use of liquid organic solvents poses a challenge for operando characterization. These solvents may cause interference in the measurements due to their strong absorption in the IR and UV/Vis spectral ranges, making it difficult to accurately monitor the catalyst behavior. Moreover, the high viscosity of liquid organic solvents may affect the mass transfer and diffusion rates of the reactants, further complicating the interpretation of the operando data. As a result, the development of appropriate operando cells and techniques for conducting characterizations with liquid organic solvents remains an active area of research.
5) *Asymmetric synthesis and hybrid SACs:* achieving enantioselectivity is essential in catalysis, and the current SACs have not been able to effectively address this issue. Recent studies have investigated the use of hybrid systems that combine enzymatic catalysis and metal SACs for asymmetric synthesis.[111] Such systems have shown potential in overcoming the current limitations of SACs and exploiting the advantages of both systems, opening new opportunities in chemistry.

To address these on-going challenges, it is indispensable to: (i) design a proper support system that comprises a well-defined and rich electronic environment capable of holding single atoms efficiently, (ii) develop and exploit SACs with high-loading of metal, and (iii) further the scope of SACs in synthetic chemistry and explore untapped reactions. We hope this review will stimulate a substantial interest among both the catalysis and synthetic communities to further investigate the use of SACs as a promising and cost-effective alternative to more expensive and sensitive catalysts, thereby fulfilling the existing and future demands of organic synthesis.

Acknowledgements

V.B.S. has received funding from the European Commission Horizon Europe programme under the Marie Skłodowska-Curie grant agreement 101064371 (SACforCO2). M.A.B was supported from the European Commission Horizon 2020 research and innovation programme under the Marie Skłodowska-Curie grant agreement 101031710 (SSEFR). G.V. has received funding from the European Commission Horizon Europe programme under the grant agreement 101057430 (SusPharma) and from the European Research Council under the grant agreement 101075832 (SAC_2.0). Open Access funding provided by Politecnico di Milano within the CRUI-CARE Agreement.

Conflict of Interest

The authors declare no conflict of interest.

Keywords: Green Chemistry · Industrial Organic Chemistry · Reactivity · Single-Atom Catalysts · Synthetic Methods

[1] a) S. Mukherjee, J. W. Yang, S. Hoffmann, B. List, *Chem. Rev.* **2007**, *107*, 5471–5569; b) D. A. Nicewicz, D. W. C. MacMillan, *Science* **2008**, *322*, 77–80; c) L. Degennaro, P. Trinchera, R. Luisi, *Chem. Rev.* **2014**, *114*, 7881–7929; d) D. Cambié, J. Dobbelaar, P. Riente, J. Vanderspikken, C. Shen, P. H. Seeberger, K. Gilmore, M. G. Debije, T. Noël, *Angew. Chem. Int. Ed.* **2019**, *58*, 14374–14378; e) S. Borgmans, S. M. J. Rogge, J. S. De Vos, C. V. Stevens, P. Van Der Voort, V. Van Speybroeck, *Angew. Chem. Int. Ed.* **2021**, *60*, 8913–8922; f) T. Kerackian, D. Bouyssi, G. Pilet, M. Médebielle, N. Monteiro, J. C. Vantourout, A. Amgoune, *ACS Catal.* **2022**, *12*, 12315–12325.

[2] Y. Xia, C. vT. Campbell, B. Roldan Cuenya, M. Mavrikakis, *Chem. Rev.* **2021**, *121*, 563–566.

[3] a) B. M. Trost, *Angew. Chem. Int. Ed.* **1995**, *34*, 259–281; b) R. H. Crabtree, *Chem. Rev.* **2015**, *115*, 127–150.

[4] a) C. Copéret, M. Chabanas, R. Petroff Saint-Arroman, J. M. Basset, *Angew. Chem. Int. Ed.* **2003**, *42*, 156–181; b) A. S. Kashin, V. P. Ananikov, *Angew. Chem. Int. Ed.* **2021**, *60*, 18926–18928; c) F. Zaera, *Chem. Rev.* **2022**, *122*, 8594–8757

[5] a) C. A. Witham, W. Huang, C.-K. Tsung, J. N. Kuhn, G. A. Somorjai, F. D. Toste, *Nat. Chem.* **2010**, *2*, 36–41; b) D. Maganas, A. Trunschke, R. Schlögl, F. Neese, *Faraday Discuss.* **2016**, *188*, 181–197; c) B. Mitschke, M. Turberg, B. List, *Chem.* **2020**, *6*, 2515–2532.

[6] a) J. Harmel, L. Peres, M. Estrader, A. Berliet, S. Maury, A. Fécant, B. Chaudret, P. Serp, K. Soulantica, *Angew. Chem. Int. Ed.* **2018**, *57*, 10579–10583; b) B. Singh, M. B. Gawande, A. D. Kute, R. S. Varma, P. Fornasiero, P. McNeice, R. V. Jagadeesh, M. Beller, R. Zboril, *Chem. Rev.* **2021**, *121*, 13620–13697; c) J. Liu, Y. Zou, D. Cruz, A. Savateev, M. Antonietti, G. Vilé, *ACS Appl. Mater. Interfaces* **2021**, *13*, 25858–25867; d) G. Vilé, P. Sharma, M. Nachtegaal, F. Tollini, D. Moscatelli, A. Sroka-Bartnicka, O. Tomanec, M. Petr, J. Filip, I. S. Pieta, R. Zbořil, M. B. Gawande, *Solar RRL* **2021**, *5*,

 © 2023 The Authors. Angewandte Chemie International Edition published by Wiley-VCH GmbH

2100176; e) J. Mosrati, A. M. Abdel-Mageed, T. H. Vuong, R. Grauke, S. Bartling, N. Rockstroh, H. Atia, U. Armbruster, S. Wohlrab, J. Rabeah, A. Brückner, *ACS Catal.* **2021**, *11*, 10933–10949.

[7] J. Fang, Q. Chen, Z. Li, J. Mao, Y. Li, *Chem. Commun.* **2023**, *59*, 2854–2868.

[8] a) M. B. Gawande, P. Fornasiero, R. Zbořil, *ACS Catal.* **2020**, *10*, 2231–2259; b) E. Lepre, S. Rat, C. Cavedon, P. H. Seeberger, B. Pieber, M. Antonietti, N. López-Salas, *Angew. Chem. Int. Ed.* **2023**, *62*, e202211663.

[9] a) Z. Jakub, J. Hulva, M. Meier, R. Bliem, F. Kraushofer, M. Setvin, M. Schmid, U. Diebold, C. Franchini, G. S. Parkinson, *Angew. Chem. Int. Ed.* **2019**, *58*, 13961–13968; b) I. S. Pieta, R. G. Kadam, P. Pieta, D. Mrdenovic, R. Nowakowski, A. Bakandritsos, O. Tomanec, M. Petr, M. Otyepka, R. Kostecki, M. A. M. Khan, R. Zboril, M. B. Gawande, *Adv. Mater. Interfaces* **2021**, *8*, 2001822; c) R. T. Hannagan, G. Giannakakis, R. Réocreux, J. Schumann, J. Finzel, Y. Wang, A. Michaelides, P. Deshlahra, P. Christopher, M. Flytzani-Stephanopoulos, M. Stamatakis, E. C. H. Sykes, *Science* **2021**, *372*, 1444–1447; d) M. G. Farpón, W. Henao, P. N. Plessow, E. Andrés, R. Arenal, C. Marini, G. Agostini, F. Studt, G. Prieto, *Angew. Chem. Int. Ed.* **2023**, *62*, e202214048.

[10] R. Qin, K. Liu, Q. Wu, N. Zheng, *Chem. Rev.* **2020**, *120*, 11810–11899.

[11] H. Jeong, S. Shin, H. Lee, *ACS Nano* **2020**, *14*, 14355–14374.

[12] Y. Li, A. I. Frenkel, *Acc. Chem. Res.* **2021**, *54*, 2660–2669.

[13] X.-F. Yang, A. Wang, B. Qiao, J. Li, J. Liu, T. Zhang, *Acc. Chem. Res.* **2013**, *46*, 1740–1748.

[14] A. Wang, J. Li, T. Zhang, *Nat. Chem. Rev.* **2018**, *2*, 65–81.

[15] S. K. Kaiser, Z. Chen, D. Faust Akl, S. Mitchell, J. Pérez-Ramírez, *Chem. Rev.* **2020**, *120*, 11703–11809.

[16] H. Gentsch, V. Härtel, M. Köpp, *Ber. Bunsenges. Phys.* **1971**, *75*, 1086–1092.

[17] a) H. Yan, C. Su, J. He, W. Chen, *J. Mater. Chem. A* **2018**, *6*, 8793–8814; b) W.-H. Li, J. Yang, D. Wang, Y. Li, *Chem* **2022**, *8*, 119–140; c) G. Giannakakis, S. Mitchell, J. Pérez-Ramírez, *Trends Chem.* **2022**, *4*, 264–276.

[18] a) P. Sharma, S. Kumar, O. Tomanec, M. Petr, J. Zhu Chen, J. T. Miller, R. S. Varma, M. B. Gawande, R. Zbořil, *Small* **2021**, *17*, 2006478; b) F. Xie, X. Cui, X. Zhi, D. Yao, B. Johannessen, T. Lin, J. Tang, T. B. F. Woodfield, L. Gu, S.-Z. Qiao, *Nat. Synth.* **2023**, *2*, 129–139.

[19] M. A. Bajada, J. Sanjosé-Orduna, G. Di Liberto, S. Tosoni, G. Pacchioni, T. Noël, G. Vilé, *Chem. Soc. Rev.* **2022**, *51*, 3898–3925.

[20] a) S. Ji, Y. Chen, X. Wang, Z. Zhang, D. Wang, Y. Li, *Chem. Rev.* **2020**, *120*, 11900–11955; b) J. Guo, H. Liu, D. Li, J. Wang, X. Djitcheu, D. He, Q. Zhang, *RSC Adv.* **2022**, *12*, 9373–9394; c) W. Li, Z. Guo, J. Yang, Y. Li, X. Sun, H. He, S. Li, J. Zhang, *Electrochem. Energy Rev.* **2022**, *5*, 9. d)

[21] C. Xia, Y. Qiu, Y. Xia, P. Zhu, G. King, X. Zhang, Z. Wu, J. Y. Kim, D. A. Cullen, D. Zheng, P. Li, M. Shakouri, E. Heredia, P. Cui, H. N. Alshareef, Y. Hu, H. Wang, *Nat. Chem.* **2021**, *13*, 887–894.

[22] Y. Chen, S. Ji, C. Chen, Q. Peng, D. Wang, Y. Li, *Joule* **2018**, *2*, 1242–1264.

[23] J. Zhang, X. Wu, W.-C. Cheong, W. Chen, R. Lin, J. Li, L. Zheng, W. Yan, L. Gu, C. Chen, Q. Peng, D. Wang, Y. Li, *Nat. Commun.* **2018**, *9*, 1002.

[24] C. Chen, W. Ou, K. Yam, S. Xi, X. Zhao, S. Chen, J. Li, P. Lyu, L. Ma, Y. Du, W. Yu, H. Fang, C. Yao, X. Hai, H. Xu, M. J. Koh, S. J. Pennycook, J. Lu, M. Lin, C. Su, C. Zhang, J. Lu, *Adv. Mater.* **2021**, *33*, 2008471.

[25] S. Liu, M. Wang, X. Yang, Q. Shi, Z. Qiao, M. Lucero, Q. Ma, K. L. More, D. A. Cullen, Z. Feng, G. Wu, *Angew. Chem. Int. Ed.* **2020**, *59*, 21698–21705.

[26] J. Xu, R. Li, C.-Q. Xu, R. Zeng, Z. Jiang, B. Mei, J. Li, D. Meng, J. Chen, *Appl. Catal. B* **2021**, *289*, 120028.

[27] T. Gan, Q. He, H. Zhang, H. Xiao, Y. Liu, Y. Zhang, X. He, H. Ji, *Chem. Eng. J.* **2020**, *389*, 124490.

[28] S. Wei, A. Li, J.-C. Liu, Z. Li, W. Chen, Y. Gong, Q. Zhang, W.-C. Cheong, Y. Wang, L. Zheng, H. Xiao, C. Chen, D. Wang, Q. Peng, L. Gu, X. Han, J. Li, Y. Li, *Nat. Nanotechnol.* **2018**, *13*, 856–861.

[29] P. Liu, Y. Zhao, R. Qin, S. Mo, G. Chen, L. Gu, D. M. Chevrier, P. Zhang, Q. Guo, D. Zang, B. Wu, G. Fu, N. Zheng, *Science* **2016**, *352*, 797–800.

[30] S. D. McCann, S. S. Stahl, *Acc. Chem. Res.* **2015**, *48*, 1756–1766.

[31] C. Zhang, C. Tang, N. Jiao, *Chem. Soc. Rev.* **2012**, *41*, 3464–3484.

[32] C. Parmeggiani, C. Matassini, F. Cardona, *Green Chem.* **2017**, *19*, 2030–2050.

[33] W. Liu, L. Zhang, X. Liu, X. Liu, X. Yang, S. Miao, W. Wang, A. Wang, T. Zhang, *J. Am. Chem. Soc.* **2017**, *139*, 10790–10798.

[34] H. Zhou, S. Hong, H. Zhang, Y. Chen, H. Xu, X. Wang, Z. Jiang, S. Chen, Y. Liu, *Appl. Catal. B* **2019**, *256*, 117767.

[35] Z. Chen, C. Liu, J. Liu, J. Li, S. Xi, X. Chi, H. Xu, I. H. Park, X. Peng, X. Li, *Adv. Mater.* **2020**, *32*, 1906437.

[36] H. Qi, L. Zhang, J. Yang, Y. Su, G. Zeng, A. Wang, T. Zhang, *J. Chem. Phys.* **2021**, *154*, 131103.

[37] D. Xu, H. Zhao, Z. Dong, J. Ma, *ChemCatChem* **2020**, *12*, 4406–4415.

[38] A. Bakandritsos, R. G. Kadam, P. Kumar, G. Zoppellaro, M. Medved', J. Tuček, T. Montini, O. Tomanec, P. Andrýsková, B. Drahoš, R. S. Varma, M. Otyepka, M. B. Gawande, P. Fornasiero, R. Zbořil, *Adv. Mater.* **2019**, *31*, 1900323.

[39] J. Büker, X. Huang, J. Bitzer, W. Kleist, M. Muhler, B. Peng, *ACS Catal.* **2021**, *11*, 7863–7875.

[40] K. Sun, H. Shan, H. Neumann, G.-P. Lu, M. Beller, *Nat. Commun.* **2022**, *13*, 1848.

[41] Z. Li, H. Li, Z. Yang, X. Lu, S. Ji, M. Zhang, J. H. Horton, H. Ding, Q. Xu, J. Zhu, J. Yu, *Small* **2022**, *18*, 2201092.

[42] E. Tiburcio, R. Greco, M. Mon, J. Ballesteros-Soberanas, J. S. Ferrando-Soria, M. López-Haro, J. C. Hernández-Garrido, J. Oliver-Meseguer, C. Marini, M. Boronat, *J. Am. Chem. Soc.* **2021**, *143*, 2581–2592.

[43] a) E. Fernández, M. A. Rivero-Crespo, I. Domínguez, P. Rubio-Marqués, J. Oliver-Meseguer, L. Liu, M. Cabrero-Antonino, R. Gavara, J. C. Hernández-Garrido, M. Boronat, A. Leyva-Pérez, A. Corma, *J. Am. Chem. Soc.* **2019**, *141*, 1928–1940; b) S. Kim, S. Jee, K. M. Choi, D.-S. Shin, *Nano Res.* **2021**, *14*, 486–492; c) H. Wei, X. Li, B. Deng, J. Lang, Y. Huang, X. Hua, Y. Qiao, B. Ge, J. Ge, H. Wu, *Chin. J. Catal.* **2022**, *43*, 1058–1065; d) S. Ji, X. Lu, M. Zhang, L. Leng, H. Liu, K. Yin, C. Xu, C. He, J. H. Horton, J. Zhang, Z. Li, *Chem. Eng. J.* **2023**, *452*, 139205.

[44] Z. Chen, E. Vorobyeva, S. Mitchell, E. Fako, M. A. Ortuno, N. Lopez, S. M. Collins, P. A. Midgley, S. Richard, G. Vile, J. Perez-Ramirez, *Nat. Nanotechnol.* **2018**, *13*, 702–707.

[45] G. Ding, L. Hao, H. Xu, L. Wang, J. Chen, T. Li, X. Tu, Q. Zhang, *Commun. Chem.* **2020**, *3*, 43.

[46] Y. Jin, F. Lu, D. Yi, J. Li, F. Zhang, T. Sheng, F. Zhan, Y. N. Duan, G. Huang, J. Dong, B. Zhou, X. Wang, J. Yao, *CCS Chem.* **2021**, *3*, 1453–1462.

[47] J. Liu, Z. X. Chen, C. B. Liu, B. Zhang, Y. H. Du, C. F. Liu, L. Ma, S. B. Xi, R. L. Li, X. X. Zhao, J. T. Song, X. Z. Sui, W. Yu, L. Miao, J. J. Jiang, M. J. Koh, K. P. Loh, *J. Mater. Chem. A* **2021**, *9*, 11427–11432.

[48] X. Zhang, Z. Sun, B. Wang, Y. Tang, L. Nguyen, Y. Li, F. F. Tao, *J. Am. Chem. Soc.* **2018**, *140*, 954–962.

© 2023 The Authors. Angewandte Chemie International Edition published by Wiley-VCH GmbH

[49] B. Hu, K. Sun, Z. Zhuang, Z. Chen, S. Liu, W. C. Cheong, C. Chen, M. Hu, X. Cao, J. Ma, R. Tu, X. Zheng, H. Xiao, X. Chen, Y. Cui, Q. Peng, Y. Li, *Adv. Mater.* **2022**, *34*, 2107721.
[50] P. Ren, Q. Li, T. Song, Y. Yang, *ACS Appl. Mater. Interfaces* **2020**, *12*, 27210–27218.
[51] Y. Zhang, S. Ye, M. Gao, Y. Li, X. Huang, J. Song, H. Cai, Q. Zhang, J. Zhang, *ACS Nano* **2022**, *16*, 1142–1149.
[52] L. Zhang, A. Wang, W. Wang, Y. Huang, X. Liu, S. Miao, J. Liu, T. Zhang, *ACS Catal.* **2015**, *5*, 6563–6572.
[53] J. Zhao, S. Ji, C. Guo, H. Li, J. Dong, P. Guo, D. Wang, Y. Li, F. D. Toste, *Nat. Catal.* **2021**, *4*, 523–531.
[54] G. Vilé, G. Di Liberto, S. Tosoni, A. Sivo, V. Ruta, M. Nachtegaal, A. H. Clark, S. Agnoli, Y. Zou, A. Savateev, M. Antonietti, G. Pacchioni, *ACS Catal.* **2022**, *12*, 2947–2958.
[55] Z. Chen, J. Song, X. Peng, S. Xi, J. Liu, W. Zhou, R. Li, R. Ge, C. Liu, H. Xu, X. Zhao, H. Li, X. Zhou, L. Wang, X. Li, L. Zhong, A. I. Rykov, J. Wang, M. J. Koh, K. P. Loh, *Adv. Mater.* **2021**, *33*, e2101382.
[56] D. Wei, C. Darcel, *Chem. Rev.* **2019**, *119*, 2550–2610.
[57] A. Maity, T. S. Teets, *Chem. Rev.* **2016**, *116*, 8873–8911.
[58] Y. Zhu, T. Cao, C. Cao, J. Luo, W. Chen, L. Zheng, J. Dong, J. Zhang, Y. Han, Z. Li, C. Chen, Q. Peng, D. Wang, Y. Li, *ACS Catal.* **2018**, *8*, 10004–10011.
[59] K. Liu, B. Badamdorj, F. Yang, M. J. Janik, M. Antonietti, *Angew. Chem. Int. Ed.* **2021**, *60*, 24220–24226.
[60] Y. Chen, S. Ji, W. Sun, W. Chen, J. Dong, J. Wen, J. Zhang, Z. Li, L. Zheng, C. Chen, Q. Peng, D. Wang, Y. Li, *J. Am. Chem. Soc.* **2018**, *140*, 7407–7410.
[61] X. Q. Feng, J. H. Guo, S. R. Wang, Q. K. Wu, Z. Chen, *J. Mater. Chem. A* **2021**, *9*, 17885–17892.
[62] B. B. Sarma, J. Kim, J. Amsler, G. Agostini, C. Weidenthaler, N. Pfander, R. Arenal, P. Concepcion, P. Plessow, F. Studt, G. Prieto, *Angew. Chem. Int. Ed.* **2020**, *59*, 5806–5815.
[63] J. Zhang, Z. Wang, W. Chen, Y. Xiong, W.-C. Cheong, L. Zheng, W. Yan, L. Gu, C. Chen, Q. Peng, P. Hu, D. Wang, Y. Li, *Chem* **2020**, *6*, 725–737.
[64] Q. Xu, C. Guo, B. Li, Z. Zhang, Y. Qiu, S. Tian, L. Zheng, L. Gu, W. Yan, D. Wang, J. Zhang, *J. Am. Chem. Soc.* **2022**, *144*, 4321–4326.
[65] W.-H. Li, J. Yang, H. Jing, J. Zhang, Y. Wang, J. Li, J. Zhao, D. Wang, Y. Li, *J. Am. Chem. Soc.* **2021**, *143*, 15453–15461.
[66] W. Xue, Z. Zhu, S. Chen, B. You, C. Tang, *J. Am. Chem. Soc.* **2023**, *145*, 4142–4149.
[67] J. F. Zhang, H. J. Zhang, Y. M. Wu, C. B. Liu, Y. Huang, W. Zhou, B. Zhang, *J. Mater. Chem. A* **2022**, *10*, 5743–5757.
[68] G. Vilé, D. Albani, M. Nachtegaal, Z. Chen, D. Dontsova, M. Antonietti, N. López, J. Pérez-Ramírez, *Angew. Chem. Int. Ed.* **2015**, *54*, 11265–11269.
[69] M. Zhou, M. Yang, X. Yang, X. Zhao, L. Sun, W. Deng, A. Wang, J. Li, T. Zhang, *Chin. J. Catal.* **2020**, *41*, 524–532.
[70] C. Chen, W. Ou, K. M. Yam, S. Xi, X. Zhao, S. Chen, J. Li, P. Lyu, L. Ma, Y. Du, W. Yu, H. Fang, C. Yao, X. Hai, H. Xu, M. J. Koh, S. J. Pennycook, J. Lu, M. Lin, C. Su, C. Zhang, *Adv. Mater.* **2021**, *33*, 2008471.
[71] Z. Li, Q. Ren, X. Wang, W. Chen, L. Leng, M. Zhang, J. H. Horton, B. Liu, Q. Xu, W. Wu, J. Wang, *ACS Appl. Mater. Interfaces* **2021**, *13*, 2530–2537.
[72] X. He, Q. He, Y. Deng, M. Peng, H. Chen, Y. Zhang, S. Yao, M. Zhang, D. Xiao, D. Ma, B. Ge, H. Ji, *Nat. Commun.* **2019**, *10*, 3663.
[73] X. Zhang, H. Lin, J. Zhang, Y. Qiu, Z. Zhang, Q. Xu, G. Meng, W. Yan, L. Gu, L. Zheng, D. Wang, Y. Li, *Chem. Sci.* **2021**, *12*, 14599–14605.
[74] W. Liu, J. Liu, X. Liu, H. Zheng, J. Liu, *ACS Catal.* **2023**, *13*, 530–539.
[75] Y. Peng, Z. Geng, S. Zhao, L. Wang, H. Li, X. Wang, X. Zheng, J. Zhu, Z. Li, R. Si, J. Zeng, *Nano Lett.* **2018**, *18*, 3785–3791.
[76] T. N. Ye, Z. Xiao, J. Li, Y. Gong, H. Abe, Y. Niwa, M. Sasase, M. Kitano, H. Hosono, *Nat. Commun.* **2020**, *11*, 1020.
[77] Z. Chen, J. Song, R. Zhang, R. Li, Q. Hu, P. Wei, S. Xi, X. Zhou, P. T. T. Nguyen, H. M. Duong, P. S. Lee, X. Zhao, M. J. Koh, N. Yan, K. P. Loh, *Nat. Commun.* **2022**, *13*, 2807.
[78] Y. Ma, Y. Ren, Y. Zhou, W. Liu, W. Baaziz, O. Ersen, C. Pham-Huu, M. Greiner, W. Chu, A. Wang, T. Zhang, Y. Liu, *Angew. Chem. Int. Ed.* **2020**, *59*, 21613–21619.
[79] H. Liu, X. Li, Z. Ma, M. Sun, M. Li, Z. Zhang, L. Zhang, Z. Tang, Y. Yao, B. Huang, S. Guo, *Nano Lett.* **2021**, *21*, 10284–10291.
[80] H. Jin, P. Li, P. Cui, J. Shi, W. Zhou, X. Yu, W. Song, C. Cao, *Nat. Commun.* **2022**, *13*, 723.
[81] X. Long, Z. Li, G. Gao, P. Sun, J. Wang, B. Zhang, J. Zhong, Z. Jiang, F. Li, *Nat. Commun.* **2020**, *11*, 4074.
[82] C. B. Liu, Z. X. Chen, H. Yan, S. B. Xi, K. M. Yam, J. J. Gao, Y. H. Du, J. Li, X. X. Zhao, K. Y. Xie, H. S. Xu, X. Li, K. Leng, S. J. Pennycook, B. Liu, C. Zhang, M. J. Koh, K. P. Loh, *Sci. Adv.* **2019**, *5*, eaay1537..
[83] L. Zhang, N. Shang, S. Gao, J. Wang, T. Meng, C. Du, T. Shen, J. Huang, Q. Wu, H. Wang, Y. Qiao, C. Wang, Y. Gao, Z. Wang, *ACS Catal.* **2020**, *10*, 8672–8682.
[84] Z. Liu, F. Huang, M. Peng, Y. Chen, X. Cai, L. Wang, Z. Hu, X. Wen, N. Wang, D. Xiao, H. Jiang, H. Sun, H. Liu, D. Ma, *Nat. Commun.* **2021**, *12*, 6194.
[85] G. Vilé, D. Ng, Z. Xie, I. Martinez-Botella, J. Tsanaktsidis, C. H. Hornung, *ChemCatChem* **2022**, *14*, e202101941.
[86] J. Gao, L. Feng, R. Ma, B.-J. Su, A. M. Alenad, Y. Liu, M. Beller, R. V. Jagadeesh, *Chem. Catal.* **2022**, *2*, 178–194.
[87] Z. Li, X. Dong, M. Zhang, L. Leng, W. Chen, J. H. Horton, J. Wang, W. Wu, *ACS Appl. Mater. Interfaces* **2020**, *12*, 57569–57577.
[88] Z. Li, L. Leng, X. Lu, M. Zhang, Q. Xu, J. H. Horton, J. Zhu, *Nano Res.* **2022**, *15*, 3114–3121.
[89] R. Lang, T. Li, D. Matsumura, S. Miao, Y. Ren, Y.-T. Cui, Y. Tan, B. Qiao, L. Li, A. Wang, X. Wang, T. Zhang, *Angew. Chem. Int. Ed.* **2016**, *55*, 16054–16058.
[90] T. Li, F. Chen, R. Lang, H. Wang, Y. Su, B. Qiao, A. Wang, T. Zhang, *Angew. Chem. Int. Ed.* **2020**, *59*, 7430–7434.
[91] J. Amsler, B. B. Sarma, G. Agostini, G. Prieto, P. N. Plessow, F. Studt, *J. Am. Chem. Soc.* **2020**, *142*, 5087–5096.
[92] P. Gao, G. Liang, T. Ru, X. Liu, H. Qi, A. Wang, F. E. Chen, *Nat. Commun.* **2021**, *12*, 4698.
[93] P. Yang, S. Zuo, F. Zhang, B. Yu, S. Guo, X. Yu, Y. Zhao, J. Zhang, Z. Liu, *Ind. Eng. Chem. Res.* **2020**, *59*, 7327–7335.
[94] W.-H. Li, B.-C. Ye, J. Yang, Y. Wang, C.-J. Yang, Y.-M. Pan, H.-T. Tang, D. Wang, Y. Li, *Angew. Chem. Int. Ed.* **2022**, *61*, e202209749.
[95] M. H. Shaw, J. Twilton, D. W. MacMillan, *J. Org. Chem.* **2016**, *81*, 6898–6926.
[96] M. Marchi, G. Gentile, C. Rosso, M. Melchionna, P. Fornasiero, G. Filippini, M. Prato, *ChemSusChem* **2022**, *15*, e202201094.
[97] a) C. Rosso, G. Filippini, A. Criado, M. Melchionna, P. Fornasiero, M. Prato, *ACS Nano* **2021**, *15*, 3621–3630; b) A. Savateev, M. Antonietti, *ACS Catal.* **2018**, *8*, 9790–9808; c) G. Gentile, M. Marchi, M. Melchionna, P. Fornasiero, M. Prato, G. Filippini, *Eur. J. Org. Chem.* **2022**, e202200944.
[98] S. Gisbertz, B. Pieber, *ChemPhotoChem* **2020**, *4*, 456–475.
[99] T. He, C. Zhang, L. Zhang, A. Du, *Nano Res.* **2019**, *12*, 1817–1823.
[100] E. Cui, H. Li, C. Zhang, D. Qiao, M. B. Gawande, C.-H. Tung, Y. Wang, *Appl. Catal. B* **2021**, *299*, 120674.

© 2023 The Authors. Angewandte Chemie International Edition published by Wiley-VCH GmbH

[101] F. Niu, W. Tu, X. Lu, H. Chi, H. Zhu, X. Zhu, L. Wang, Y. Xiong, Y. Yao, Y. Zhou, Z. Zou, *ACS Catal.* **2022**, *12*, 4481–4490.
[102] Q. Wang, J. Li, X. Tu, H. Liu, M. Shu, R. Si, C. T. J. Ferguson, K. A. I. Zhang, R. Li, *Chem. Mater.* **2020**, *32*, 734–743.
[103] J. Ma, F. Zhang, Y. Tan, S. Wang, H. Chen, L. Zheng, H. Liu, R. Li, *ACS Appl. Mater. Interfaces* **2022**, *14*, 18383–18392.
[104] M. Kwak, J. Bok, B.-H. Lee, J. Kim, Y. Seo, S. Kim, H. Choi, W. Ko, W. Hooch Antink, C. W. Lee, G. H. Yim, H. Seung, C. Park, K.-S. Lee, D.-H. Kim, T. Hyeon, D. Yoo, *Chem. Sci.* **2022**, *13*, 8536–8542.
[105] Z. Chen, J. Liu, M. J. Koh, K. P. Loh, *Adv. Mater.* **2022**, *34*, 2103882.
[106] Y. Hu, H. Li, Z. Li, B. Li, S. Wang, Y. Yao, C. Yu, *Green Chem.* **2021**, *23*, 8754–8794.
[107] B. Wang, P. Zhou, X. Yan, H. Li, H. Wu, Z. Zhang, *J. Energy Chem.* **2023**, *79*, 535–549.
[108] H. Zhang, X. Zhang, S. Shi, Q. He, X. He, T. Gan, H. Ji, *ACS Appl. Mater. Interfaces* **2022**, *14*, 53755–53760.
[109] J. Xia, B. Wang, J. Di, Y. Li, S.-Z. Yang, H. Li, S. Guo, *Mater. Today* **2022**, *53*, 217–237.
[110] W. Sangkhun, J. Ponchai, C. Phawa, A. Pengsawang, K. Faungnawakij, T. Butburee, *ChemCatChem* **2022**, *14*, e202101266.
[111] X. Li, Y. Cao, J. Xiong, J. Li, H. Xiao, X. Li, Q. Gou, J. Ge, *Chin. J. Catal.* **2023**, *44*, 139–145.

Manuscript received: December 30, 2022
Accepted manuscript online: March 14, 2023
Version of record online: ■■, ■■

© 2023 The Authors. Angewandte Chemie International Edition published by Wiley-VCH GmbH

Reviews

Catalysis

V. B. Saptal, V. Ruta, M. A. Bajada, G. Vilé* **e202219306**

Single-Atom Catalysis in Organic Synthesis

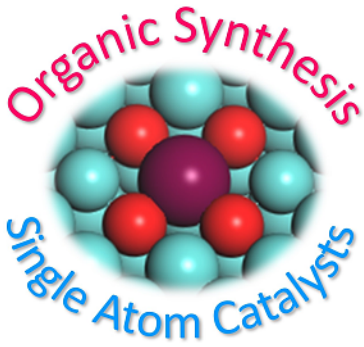

Single-atom catalysts, featuring atomically dispersed metals on solid carriers, offer limitless possibilities for new, sustainable transformations in the chemical sector. These materials bridge the gap between organometallic and nanoparticle catalysis and are opening exciting avenues for mimicking metalloenzymes. This Review summarizes the impressive progress and potential knowledge gaps in the use of single-atom catalysts in organic synthesis.

© 2023 The Authors. Angewandte Chemie International Edition published by Wiley-VCH GmbH